Tunnel valleys of the central and northern North Sea (56°N to 62°N): distribution and characteristics

Ottesen, D.[1], Stewart, M.[2], Brönner, M.[1,3], Batchelor, C.L.[3]

[1] Geological Survey of Norway, P.O. Box 6315 Torgarden, N-7491 Trondheim, Norway;
[2] British Geological Survey, The Lyell Centre, Research Avenue South, Edinburgh EH14 4AP, UK;
[3] Norwegian University of Science and Technology, Department for Geoscience and Petroleum, N-7491 Trondheim, Norway;
[4] Scott Polar Research Institute, University of Cambridge, Cambridge CB2 1ER, UK.

ABSTRACT

The analysis of buried tunnel valleys in the North Sea can provide information about the past configuration and dynamics of the Scandinavian and British ice sheets and the processes by which sediment and meltwater were transported at the ice-sheet base. However, little is presently known about the distribution and characteristics of tunnel valleys in the Norwegian sector of the North Sea. Here we use an extensive database of 3D seismic and high-resolution magnetic data to map more than 2200 tunnel valleys in the Norwegian and British sectors of the North Sea between 56°N and 62°N. With the exception of the deep Norwegian Channel, in which evidence for tunnel valleys is absent, the geological setting of the North Sea is interpreted to have been conducive to tunnel-valley formation and preservation because of its poorly consolidated substrate and shallow water depths. The highest density of tunnel valleys is located in the central part of the North Sea where Quaternary sediments are thickest. The extreme length of some of the tunnel valleys, which are up to 155 km long, supports theories that tunnel valleys form in stages rather than catastrophically. Detailed analysis of the orientation of tunnel valleys and their relative age relationships within four representative subareas shows that tunnel-valley orientation varies significantly across the central and northern North Sea and between different generations of valleys. This suggests that the pattern of subglacial meltwater drainage in the central and northern North Sea was different between each deglacial event in which tunnel valleys were formed.

1. INTRODUCTION

Tunnel valleys are elongated and over-deepened depressions eroded by subglacial water flow into underlying sediments or bedrock under high water-pressure (Ó Cofaigh, 1996; Benn and Evans, 2010; Kehew et al., 2012; van der Vegt et al., 2012). Tunnel valleys often start and terminate abruptly and are found buried and with surface expression, both onshore and offshore. They are often found in soft, poorly consolidated substrates, which are susceptible to erosion by water, but they can also appear in areas of harder substrate (Stackebrandt, 2009; Sandersen and Jørgensen, 2012), where they are sometimes associated with eskers. Tunnel valleys can reach lengths of more than 100 km, widths of up to 10 km and depths of 500 m (Ó Cofaigh, 1996; Huuse and Lykke-Andersen, 2000; Praeg, 2003; Lutz et al., 2009; Stackebrandt, 2009; van der Vegt et al., 2012). In plan-form, tunnel valleys are observed as individual straight or sinuous channels, and as complex anastomosing or dendritic networks (Praeg, 2003). A significant morphological characteristic of tunnel valleys is the presence of an undulating longitudinal profile, which is indicative of a subglacial origin by meltwater under pressure (van der Vegt et al., 2012).

Pleistocene tunnel valleys are found in many areas of the formerly glaciated world, but have most often been reported from northern Europe and North America both on and offshore (Wright, 1973; Shaw and Gilbert, 1990; Piotrowski, 1997; Huuse and Lykke Andersen, 2000; Praeg, 2003; Lutz et al., 2009; Stackebrandt, 2009; Hepp et al., 2012; van der Vegt et al., 2012, Livingstone and Clark, 2016; Coughlan et al., 2018; Montelli et al., 2020; Winsemann et al., 2020) where they formed beneath the ice sheets that existed during Quaternary glacial periods. Tunnel valleys can contain important reservoirs for water or hydrocarbons (Huuse and Lykke-Andersen, 2000; Praeg, 2003), and can also contain shallow gas that can cause problems for seabed installations and hazards for drilling. The valleys also affect seismic imaging with depth due to the lithological variations of the infilled sediments.

Generally, tunnel valleys are considered most likely to develop in the marginal, low-altitude zone of continental ice sheets, and are linked to the production of surface meltwater that reaches the ice-sheet bed. Subglacial drainage develops relating to whether water can be transported through the subsurface, along the ice-sheet bed, or within channels or other drainage pathways such as tunnel valleys. In general, tunnel-valley formation is considered to occur where meltwater influx is substantial (likely during deglacial periods, or ice-sheet retreat), leading to subglacial conditions that encourage the formation of channel systems (Boulton and Hindmarsh, 1987; Boulton et al., 2009). How the channel systems are formed depends on substrate permeability, conditions at the ice-sheet bed (frozen or melting), influx of meltwater (and therefore climatic variations and ice thickness), and the topography beneath

the ice sheet (see van der Vegt et al., 2012 and references therein). The majority of the tunnel valleys previously studied in the central and northern North Sea are considered to have formed in unconsolidated or poorly consolidated relatively soft substrate which was repeatedly over-ridden by ice (Graham et al., 2011).

There are three main theories of tunnel-valley formation (Kehew et al., 2012; van der Vegt et al., 2012): (i) steady-state subglacial drainage of meltwater along hydrostatic pressure gradients; (ii) catastrophic meltwater discharge; (iii) direct glacial erosion with meltwater as the most important erosional agent. A combination of the above formation methods may also be considered, with evidence for complex formation over time, re-occupation and later alteration (such as cut and fill structures and internal clinoforms) (Kristensen et al., 2007; Huuse and Lykke-Andersen, 2000; Stewart et al., 2013; Winsemann et al., 2020). Moreau and Huuse (2014), for example, find evidence for tunnel valley fill by post-glacial fluvial sediments, whereas Praeg (2003) and Benvenuti et al. (2018) describe backfill of tunnel valleys during their formation process.

Tunnel-valley orientation is often described as perpendicular to the ice margin, and sub-parallel to the direction of past ice flow (Huuse and Lykke-Andersen, 2000; van der Vegt, 2012). Praeg (2003) and Stackebrandt (2009), for example, describe generally southwards-trending tunnel valley systems in the southern North Sea and in Germany, which the authors relate to the southern edge of the Elsterian (Marine Isotope Stage (MIS) 12) ice margin.

However, other recent studies find evidence for E – W trending tunnel valleys in the southern North Sea and onshore northern Europe (Lutz et al., 2009; Hepp et al., 2012; Müther et al., 2012; Coughlan et al., 2018; Winsemann et al., 2020), and recent work by Lelandais et al. (2016) shows tunnel valleys forming parallel to ice margins in model conditions. In the central and northern North Sea, tunnel valleys are also observed with a variety of orientations (Kristensen and Huuse, 2012; van der Vegt et al., 2012; Stewart and Lonergan, 2011; Stewart et al., 2013), making a clear link to ice-sheet margins less obvious. The only previous study of tunnel valleys in the Norwegian sector of the North Sea was performed by Fichler et al. (2005), in which tunnel valleys in an area centred on 59°N, 2°E were mapped using 3D seismic cubes and high-resolution magnetic data and display a variety of orientations.

In the North Sea region, three generations of tunnel valleys have been recognised by many researchers both on and offshore, with each generation being correlated to one of the three last major glaciations on land in the surrounding countries: The Elsterian (MIS 12), Saalian (MIS ?10 - 6), and Weichselian (MIS 5d – 2) (Ehlers and Linke, 1989; Wingfield,

1989, 1990; Kluiving et al., 2003). More recently, with the availability of extensive 3D seismic data , the complex pattern of tunnel valleys observed offshore reveal that a simple correlation between tunnel-valley formation and a threefold glaciation history is too simple; rather, the complex networks of tunnel valleys comprise multiple sets or 'generations' of cross-cutting tunnel valleys. Kristensen et al. (2007) identified at least five tunnel-valley generations, whilst Stewart and Lonergan (2011) and Stewart et al. (2013) mapped up to seven generations of buried tunnel valleys in the central North Sea.

The oldest tunnel valleys in the North Sea and northern central Europe are often described in the literature as Elsterian (MIS 12), but these ages are generally considered to be poorly constrained due to paucity of stratigraphic age data (Huuse and Lykke-Andersen, 2000; Lutz et al., 2009; Müther et al., 2012). Further complexity is added by studies which show evidence for re-occupation or overprinting of tunnel valleys during subsequent glaciations, for example, that of Müther et al. (2012) in the Danish North Sea. Recent work by Roskosch et al. (2015), using Optically Stimulated Luminescence (OSL) dating, suggests an MIS 10 age for tunnel valley fill in northern Germany, later re-occupied during the Saalian (MIS 6). Glaciogenic sediments from Germany and the Netherlands also suggest that ice sheets occupied at least part of the North Sea during MIS 8 (Laban and van der Meer, 2011; Roskosch et al., 2015).

In the central and northern North Sea, very little data is available to constrain the ages of the buried tunnel valleys investigated in this study. In general, the buried tunnel valleys are described by Stewart and Lonergan (2011) and Stewart et al. (2013) as younger than the Brunhes-Matuyama palaeo-magnetic reversal event at 780 ka (Stoker et al., 1983), and older than the Last Glacial Maximum at 22.7 – 19.2 ka; the latter date is based on material from the British Geological Survey (BGS) borehole 77/03, which was dated by Sejrup et al. (1994), and from nearby borehole 04/01, dated by Graham et al. (2010). The oldest valleys are considered to be MIS 12 in age based on Toucanne et al. (2009), who date the first influx of glacially influenced meltwater to the Bay of Biscay at MIS 12. However, it is possible that the oldest tunnel valleys pre-date MIS 12, with evidence for ice advances across the North Sea from MIS 34 in the German and Dutch sectors, and from MIS 16 in the UK (see Lee et al., 2012 and references therein).

In this study we map all the tunnel valleys which we were able to discern in the Norwegian and British sectors of the North Sea north of 56°N, based on a large database of 3D seismic (>100,000 km^2) and high-resolution aeromagnetic data (Fig. 1). We analyse

tunnel-valley morphology and establish a relative age relationship between the tunnel valleys in four representative subareas. The orientations and density of the tunnel valleys are discussed in terms of geological and glaciological controls on the formation and preservation of tunnel valleys in the central and southern North Sea, and their implications for the routing of subglacial meltwater during regional deglaciation.

2. GEOLOGICAL BACKGROUND

The North Sea Basin has experienced significant deposition from the Jurassic onwards. During the Cenozoic, up to 3,000 m of sediments filled the central parts of the basin, resulting in subsidence along the basin axis (Gatliff et al., 1994). The basin, which extends towards the east into Germany and Poland, was gradually infilled by sediments during the Miocene/ Pliocene (Stackebrandt, 2009; Thøle et al., 2014). The BGS undertook extensive regional mapping of the Quaternary stratigraphy of the entire British shelf during the 1970s and 1980s based on analogue 2D seismic lines and boreholes. In the southern North Sea, the lower part of the Quaternary basin is infilled by relatively fine-grained deltaic sediments sourced from the east (Gatliff et al., 1994; Overeem et al., 2001). The lithology of the early Quaternary infill of the central to northern North Sea comprises mainly glacimarine to marine sediments composed predominantly of sandy muds with some gravel and occasional sand layers (Stoker, 1987; Johnson et al., 1993; Gatliff et al., 1994). Lamb et al. (2016) describe early Quaternary marine silty claystones based on gamma log data and well cuttings from two wells (22/25a-3 and 30/6-3) in the UK sector.

More recently, the availability of 2D and 3D seismic data from the North Sea has enabled detailed reconstructions of the evolution of the basin through the Quaternary (Lamb et al., 2017; Ottesen et al., 2018). In the northern North Sea (59-62ºN), the lower part of the Quaternary basin is infilled by a series of prograding sedimentary units (mainly glacigenic debris-flows originating from the delivery of subglacial sediment to the palaeo-shelf break) deposited from the east/southeast towards the west/northwest (Ottesen et al., 2014; Batchelor et al., 2017). The top of these units is cut by a prominent unconformity, which is termed the Upper Regional Unconformity (URU) (Moreau et al., 2012). In the east, the URU represents the base of the Norwegian Channel (Fig. 1), which was produced by erosion from the recurrent Norwegian Channel Ice Stream from around 1 Ma (Sejrup et al., 1995; Ottesen et al., 2014). West of the Norwegian Channel, the URU separates clinoforms deposited from the east and clinoforms sourced from the west.

In the central North Sea, a Quaternary sedimentary sequence up to 1,000 m thick filled in the deepest parts of the basin (Fig. 2) (Lamb et al., 2017; Ottesen et al., 2018). Sediment sources were mainly from the southeast by fluvial input as an elongated deltaic depocentre from the palaeo-Baltic river system. Some sediments were also sourced from the large European rivers, such as the Rhine-Meuse, and from the northeast (Norway) and west (UK) by fluvial/glacifluvial processes (Gibbard, 1988). In the central North Sea, the URU surface, which was originally mapped and extended from the northern North Sea, is represented as a conformity separating several relatively flat-lying units (Fig. 2) (Ottesen et al., 2014). Tunnel valleys appear mostly in these uppermost flat-lying units above the URU, to approximate depths of around 400 m beneath the seabed. In agreement with Stewart and Lonergan (2011) and Stewart (2016), the distribution of tunnel valleys in our study area is not influenced by bedrock or other subsurface structures (such as salt domes).

The depositional environment of the Quaternary North Sea was complex, varying from subglacial to subaerial or proglacial, lacustrine or shallow marine. As water depth in the basin generally shallowed through the Quaternary as the basin became infilled, subaerial exposure linked to glacio-eustatic changes during Quaternary glaciations became more likely. Despite the use of industry 3D seismic data to interpret landforms on palaeo-surfaces within the stratigraphy of the basin (Stuart and Huuse, 2012; Dowdeswell and Ottesen, 2013; Ottesen et al., 2014, 2016; Lamb et al., 2016, 2017; Rose et al., 2016; Stewart, 2016; Batchelor et al., 2017; Reinardy et al., 2017; Rea et al., 2018), uncertainty still remains about the configuration, timing and extent of ice sheets in the North Sea. The relative stratigraphy of tunnel valleys has been used to consider the total number of ice-sheet advances that have affected the basin during the Quaternary (Stewart and Lonergan, 2011), although a lack of absolute dates, complex tunnel-valley patterns, re-occupation of older tunnel valleys by younger tunnel valleys, and a relatively poor understanding of the formation processes for tunnel valleys have made interpretation difficult. Most often, a conceptual model with an ice sheet covering the North Sea during the last three major glaciations (Weichselian, Elsterian and Saalian) are generally described, but this has been questioned, first by Stewart and Lonergan (2011), who found up to seven tunnel-valley generations potentially relating to MIS indicative of cold periods, and subsequently by other authors (e.g. Winsemann et al., 2020). Tunnel valleys provide unequivocal evidence of ice-sheet cover because they are formed subglacially. However, it is not clear exactly how generations of tunnel valleys relate to ice-sheet advances and readvances within a single glacial period.

The identification of iceberg ploughmarks on horizons dated to older than 2 Ma in the southern and central North Sea (Dowdeswell and Ottesen, 2013; Rea et al., 2018) and glacigenic debris-flows on palaeo-slope surfaces close to the base-Quaternary in the northern North Sea (Ottesen et al., 2014, 2018; Batchelor et al., 2017) has pushed the glacial history of the North Sea back to the beginning of the Quaternary. Although it is possible that some of these earlier glaciations resulted in tunnel-valley formation, most of the thousands of buried tunnel valleys that are preserved within the flat-lying sediment units above the URU (Fig. 2) are younger than 1 Ma in age, by which time the North Sea Basin was mainly infilled (Ottesen et al., 2018).

3. DATABASE AND METHODS

Our study area comprises the Norwegian and British sectors of the North Sea north of 56°N (Fig. 1). We merged the mapping carried out by Lonergan et al. (2006), Stewart and Lonergan (2011) and Stewart et al. (2012) with extensive new mapping of tunnel valleys in the Norwegian sector of the North Sea. The boundary of the study area follows approximately the western limit of the 3D seismic cubes, whereas in the east the limit is set 10 to 20 km outside the Norwegian coastline close to the boundary between crystalline and sedimentary rocks (Fig. 1). To the north, the study area is bounded by the limit of the 3D seismic cubes at around 62°N. The study region has a total area of approximately 180,000 km^2.

3.1 3D seismic database

The PGS Megasurvey comprises most of the released 3D seismic reflection cubes of the Norwegian part of the North Sea (56°N-62°N) and many cubes in the British sector (Fig. 1), which have been merged together. The Megasurvey is organised into rectangles, where individual 3D cubes have been merged and clipped inside each of the rectangles (Fig. 3a). Each rectangle is composed of many 3D cubes with variations in seismic acquisition directions (white lines in Fig. 3a).

The quality of the seismic data is variable across the merged dataset (e.g. Fig. 3b). As the 3D surveys were configured to image the subsurface at greater depths than examined here, the upper parts of the merged seismic cubes sometimes display a poor signal to noise ratio, and the contrast in acoustic impedance between seabed and water column can cause disruption close to this interface (Fig. 3b). Data gaps are also visible (Fig. 3a and b). However, as in other studies (Lonergan et al., 2006; Kristensen et al., 2007; Lutz et al., 2009; Kristensen and Huuse, 2012; Moreau et al., 2012; Muther et al., 2012; Stewart et al., 2012,

2013), the ability to explore 3D seismic reflection data both vertically and horizontally allows comprehensive imaging of laterally complex features, such as tunnel valleys, across the region, even in the shallower sections of the 3D data. Areas of relatively poor seismic data within our study area are highlighted in yellow in Figure 4.

The vertical sampling interval for the PGS Megasurvey is 4 ms (c. 3 m), which provides a maximum vertical resolution. Horizontal resolution for the entire merged survey is 25 m, a considerable improvement on previous regional merged datasets in which the outlines of tunnel valleys could be observed but no further detail was visible (e.g. Stewart et al., 2013).

The Utstord cube, to the east of the PGS Megasurvey (AOI 2 in Fig. 1), has a horizontal resolution of 25 m and vertical sampling every 4 ms. Acquisition direction is NNW-SSE. Some additional 3D seismic cubes outside (or partly overlapping) the PGS Megasurvey are used (Fig. 1) (e.g. TA0701, NH0504, EGB 2005, NVG-10M, and TT933F001). In total, *c.* 110 000 km^2 are covered by 3D seismic data.

3.2 High-resolution aeromagnetic data

During the Geological Survey of Norway's (NGU) Crustal Onshore-Offshore Project (COOP; Olesen et al., 2013), an updated airborne magnetic survey map was compiled from existing and new high-resolution magnetic data (Figs. 1 and 4). Approximately 82,000 km of new aeromagnetic data was acquired in the Norwegian North Sea (CNAS-10) in a regular line-tie-line configuration with 1 km line spacing and a sensor altitude of 115 m above sea-level. These data were merged with existing magnetic data from TGS (VGVG-96, Q-17 and the UHAM-09), which were acquired at a similar altitude but with denser line spacing of 200 to 250 m, and approximately 50 m lateral resolution.

High-pass filtering was applied to the new magnetic data compilation to extract the magnetic signal from shallow sources and to highlight the signature of the tunnel valleys. The high-pass filtered data also reflect the varying resolution of the different surveys, which is mainly related to acquisition parameters including flight altitude and profile distance. Increases in water depth and distance-to-magnetic source decrease the signal-to-noise ratio and can hamper channel identification.

3.3 Mapping of tunnel valleys

3.3.1 Seismic data

The 3D seismic cubes were inspected for tunnel valleys using mainly horizontal timeslices through the surveys in which tunnel-valley margins are well-imaged (Figs. 5 to 8). Initial screening for tunnel valleys was carried out from the seabed at intervals of 50 ms in timeslice, and the margins of the valleys were digitised using Petrel seismic interpretation software before being exported to ESRI ArcGIS.

From this initial reconnaissance, four Areas of Interest (AOI) were selected for closer inspection (Figs. 1, 5 to 8) using the 3D seismic data. The AOI were selected based on data quality (i.e. that tunnel valleys were well-imaged within the volume) and to provide representative examples of tunnel valleys across the region, as well as to complement the study areas of previous work. AOI 1 was chosen to show the buried valleys in the southern part of the study area, and to expand on the work carried out by Stewart et al. (2013, see their 'Dataset M', Fig. 1a). AOI 2 was chosen due to its location in the easternmost part of the North Sea Plateau close to the Norwegian Channel, and because it is covered by a high-quality 3D seismic cube (Utstord Cube, Fig. 1) which provided very good imaging of the tunnel valleys. AOI 3 was selected because of its northern location and the presence of some unusual N-S-trending tunnel valleys. AOI 4 was chosen based on its westerly location, the comparatively high density of tunnel valleys present, and the location of previous interpretations by Stewart and Lonergan (2011) and Stewart et al. (2013, see their 'Datasets A-G', Fig. 1a).

The margins of the tunnel valleys within these AOI were mapped in timeslices at 4 to 8 ms intervals. Further detailed measurements of individual tunnel-valley morphology (width, length, orientation) were performed in ArcMap using these digitised horizons. Circular statistical analyses and calculation of mean resultant directions were performed using the GeOrient software. All orientation measurements are presented as bidirectional because flow direction for tunnel-valley formation has not been consistently established.

In the four AOI (Figs. 5-8), cross-cutting relationships and geomorphological similarity between tunnel valleys, imaged in horizontal timeslices, were used to group the tunnel valleys into 'generations' considered to be of a similar age, using the method described in Stewart and Lonergan (2011) and in Figure 6 of Stewart et al. (2013). In AOI 1 and AOI 4, generational interpretations first described in Stewart and Lonergan (2011) and Stewart et al. (2013) were expanded further using the new PGS Megasurvey seismic data. Mean orientations were calculated for individual generations as above.

3.3.2 Magnetic data

State-of-the-art high-resolution magnetic data enable the identification of subtle magnetization contrasts both onshore and offshore. The only limiting factors are distance to the source and data density, which control the lateral resolution of the data. The disturbance of sedimentary layers due to erosion and subsequent infill of new sediments can produce significant magnetic contrasts even in generally low magnetic sediments. Magnetic data are commonly utilised in archeology to identify buried ancient settlements; for example, former grabens and ditches for houses or palisades that have been buried by sediment often produce a regular pattern in magnetic data (e.g. Kvamme, 2003).

The same principle can be used, at a larger scale, to identify buried tunnel valleys in the offshore record (Fichler et al., 2005). There is a subtle but detectable magnetization contrast between the sediments that were eroded by subglacial meltwater to form a tunnel valley and the heterogenic infill of the valley (Olesen et al., 2010; Brahimi et al., 2019). In addition, a secondary change in magnetic mineralogy may result from biological and chemical differences between the sediments. High-pass filtered magnetic data emphasize these contrasts and can resolve several generations of tunnel valleys at different depths (Fichler et al., 2005; Brahimi et al., 2019).

In our aeromagnetic data, Quaternary tunnel valleys are imaged clearly as both positive and negative anomalies (Fig. 3c). At the first order, positive magnetic anomalies are likely to be produced where a tunnel valley is infilled by relatively coarse-grained sediment dominated by basement clasts that have a significantly higher magnetization compared to surrounding sedimentary rocks (Olsen et al., 2010). Negative anomalies are probably produced where a tunnel valley is infilled by relatively fine-grained sand, silt and clay that have lower magnetization compared to the base and sides of the tunnel valley. Although the magnitude of these contrasts is typically small, because quartz-dominated fine-grained sediments commonly show low magnetization, state-of-the-art magnetometers and high-density data acquisition enable channels with this type of infill to be mapped (Fig. 3c).

Where no seismic data are available (Fig. 1), we interpreted channel features from the magnetic data only. Although the mapping of tunnel valleys based solely on magnetic data might not detect the entire system, the aeromagnetic data provide an overview of the distribution of the channels (Fig. 4). For channels that display a relatively straight geometry, it can be difficult to differentiate tunnel valleys from other source anomalies, including pipelines, cables and sub-crops of sedimentary layers. In addition, data artefacts, such as those reflecting the direction of data acquisition, can appear similar to relatively linear channels. To avoid over-interpretation of magnetic lineaments in our analysis of the high-pass filtered

magnetic data, the dendritic or slightly meandering shape of magnetic anomalies (Fig. 3c) was used as a character identifier of tunnel valleys.

Overall, we identify several cross-cutting channel systems from the magnetic data (Fig. 4). Where both types of data are available, we find the use of seismic and magnetic data to detect tunnel valleys to be well-correlated (Fig. 9).

4. RESULTS

4.1 General distribution and morphology

A total of 2297 tunnel valleys were mapped across an area of approximately 150,000 km^2 in the British and Norwegian sectors of the North Sea; 2158 tunnel valleys in 3D seismic data, and 139 in the magnetic surveys only (Fig. 4). The tunnel valleys have a combined length of more than 33,000 line-km. All of the tunnel valleys are 0.5-10 km wide and tens to hundreds of meters in depth, which is consistent with nearby studies compiled by van der Vegt et al. (2012) and Stewart et al. (2013).

Some of the valleys have surface expression, and are known from bathymetric surveys (i.e. Stewart, 2016), but most described here are buried. The majority of the tunnel valleys are imaged between the seabed and around 600 ms two-way travel time (TWT), equivalent to around 400 m beneath the seabed using sediment velocities of 1700-1900 m/s (Graham, 2007; Ottesen et al., 2014), generally deepening to the south. A map of tunnel-valley density, which was calculated using the mapped valleys in both the seismic and magnetic datasets, shows that the highest density of tunnel valleys is in the center of the study area at around 1.7°E, from 59°N to 59.2°N, although this is partly reliant on data coverage and quality (Fig. 10). Buried tunnel valleys are observed north of 61°N, which has not been reported previously in the North Sea. Although this area is covered by our magnetic dataset, no tunnel valleys are reported from within the Norwegian Channel (Figs. 4 and 10).

The most striking geomorphological observation from our new regional cross-border dataset is the length of the buried tunnel valleys; the longest feature is measured at 155 km, and this is limited by data extent (Fig. 11). To our knowledge, this is the longest tunnel valley observed in the North Sea to date. At least two other buried tunnel valleys are measured at >100 km in length, and several valleys are observed with lengths of 80-100 km (Fig. 11). It is likely that these measurements are underestimating true lengths, partly due to data coverage and also because areas of poor data quality within the merged 3D datasets preclude the correlation of valleys between regions (Figs. 1, 4 and 10).

As observed in previous works (Lonergan et al., 2006; Kristensen et al., 2007; Lutz et al., 2009; Stewart and Lonergan, 2011; Muther et al., 2012; Stewart et al., 2013), the complex system of tunnel valleys mapped across the North Sea comprises numerous overlapping systems that can be separated into a number of 'generations' of varying age. Below, we describe the morphology and generational interpretation (with 'Generational 1' as the oldest) of tunnel valleys in more detail for AOI 1 to 4 across the study area (Figs. 5-8).

4.2 Area of Interest 1

AOI 1 is situated in the southern part of the study area from 56.30°N, 2.12°E to 57.21°N, 3.08°E (Fig. 1). The total study area is 4500 km^2. From the PGS Megasurvey 3D seismic data, we identified fifteen valleys that could be well-defined and/or mapped within the interpretation software (Fig. 5). Many of the valleys appear to extend outside the study area, although some shorter valleys begin and terminate within the AOI and have lengths of around 25-30 km.

AOI 1 extends the area interpreted as 'Dataset M' in Figure 9 of Stewart et al. (2013), enabling the additional tunnel valleys that we observe here to be analysed in the generational framework outlined by those authors. Five cross-cutting generations of tunnel valleys are observed in AOI 1 (Fig. 5). Weighted orientation measurements (Table 1) show that the two oldest sets of tunnel valleys (generations 1 and 2) generally trend NE-SW while the youngest three sets display a pronounced NW-SE preferred orientation (Fig. 5c). Of note in AOI 1 is the large set of NW-SE trending youngest valleys (Generation 5, pink in Fig. 5), which display significant anastomosing sections and clearly cross-cut older generations (Fig. 5d). The largest of these valleys likely extends beyond AOI 1 and reaches a length of up to 155 km (Fig. 11).

4.3 Area of Interest 2

AOI 2 is defined by the Utstord 3D seismic reflection cube, which is located in the transition zone between the North Sea Plateau and the Norwegian Channel, from 58.47°N, 2.30°E to 59.41°N, 3.59°E (Fig. 1). The seismic cube covers an area of 5285 km^2. Of this, *c.* 2900 km^2 (57 %) covers the North Sea Plateau, and the rest the Norwegian Channel (Fig. 6b). Many of the valleys within AOI 2 appear to terminate, or are roughly perpendicular, towards the flank of the Norwegian Channel (Fig. 6b). Although tunnel valleys are not identified within the channel itself, a few valleys extend onto its western margin (Fig. 4).

Around 25 tunnel valleys were identified within AOI 2, although only 6 clearly cross-cut one another; these were interpreted as forming five generations (Fig. 6b and c). Some of the older valleys are clearly incising from a lower stratigraphic level than the youngest (Fig. 6d). The defining characteristic of the AOI 2 tunnel valleys, including those not included in the generational framework (grey in Fig. 6), is their general NE-SW trend, with only a few valleys, in generations 1 and 3, displaying a more preferred NNE-SSW and NNW-SSE directionality, respectively (Fig. 6b and c, Table 1). Given the relatively low number of valleys that cross-cut one another in this AOI, overall patterns of directionality in the generational interpretation (summarised in Table 1) are not considered to be as significant as in some other areas. However, the NE-SW trend of the majority of the valleys is likely related to their proximity to the Norwegian Channel, which is discussed further in Section 5.

4.4 Area of Interest 3

AOI 3 is situated in the north-eastern part of the study area from 60.09°N, 1.53°E to 60.71°N, 2.04°E (Fig. 1). The total study area is 2460 km^2. From the PGS Megasurvey 3D seismic data, 9 tunnel valleys are relatively well-imaged, although data quality in this area is comparatively poor (Fig. 7a). Five cross-cutting generations of tunnel valleys are identified (Fig. 7b). Many of the valleys appear to extend beyond the AOI boundary; the two large N-S trending tunnel valleys, which are assigned to generations 3 and 4, are >80 km in length (Fig. 7b). Figure 7d shows a seismic profile across these two tunnel valleys in 3D seismic survey TT 933F001, but the presence of a strong seabed multiple obscures the detail of the tunnel-valley margins to some extent. The N-S directionality of these two tunnel valleys (Table 1) appears to be quite unusual across the whole study area, but is more common north of 60°N (Fig. 4).

4.5 Area of Interest 4

AOI 4, which is located in the western part of the study area within the UK sector of the North Sea Plateau from 58.06°N, 0.61°W to 58.61°N, 0.28°E (Fig. 1), has a total area of 3090 km^2. From the PGS Megasurvey 3D seismic data, we identified 23 well-defined tunnel valleys that could be mapped in the interpretation software and placed within a generational context (Fig. 8). Almost all of the valleys appear to extend beyond the study area (Fig. 8b).

Our interpretation of the tunnel valleys in AOI 4 builds upon the work of Stewart et al. (2013, their Datasets A-G) to the northwest of the study area. Here, previous and new mapping of tunnel valleys inform a new interpretation of cross-cutting relationships. This

study, with a minimum horizontal resolution of 25 m, allows interpretation across previously unresolvable areas as well as the imaging of the tunnel valleys in greater detail (see Fig. 1b and Fig. 8 of Stewart et al., 2013 compared to Fig. 8 of this study). As in Stewart and Lonergan (2011) and Stewart et al. (2013), we find seven generations of cross-cutting buried tunnel valleys in this area (AOI 4). Tunnel-valley orientations in AOI 4 are summarised in Table 1, with the oldest generations, 1 to 3, showing a preferred NNE-SSW orientation. Generations 5 and 7 show a NE-SW trend, while generations 4 and 6 are less strongly oriented (Fig. 8c).

5. DISCUSSION

This study shows that buried tunnel valleys are present extensively across the British and Norwegian sectors of the central and northern North Sea, extending eastwards to the western margin of the Norwegian Channel (Fig. 4) and north towards the continental shelf break. In agreement with previous research in smaller study areas (van der Vegt et al., 2012; Stewart et al., 2013), the tunnel valleys can be separated into several cross-cutting generations (Figs. 5-8). Below, we discuss a number of points from this new work.

5.1 Tunnel-valley generations

Five generations of cross-cutting tunnel valleys are described in AOI 1 to 3, and seven in AOI 4 (Figs. 5-8), which is consistent in number to those observed in other central and southern North Sea studies using 3D seismic data (Lonergan et al., 2006; Kristensen et al., 2007; Lutz et al., 2009; Stewart and Lonergan, 2011; Müther et al., 2012; Stewart et al., 2013). The complexity of the tunnel-valley systems in our AOI, which are separated by distances of >150 km, combined with gaps in data coverage and areas of lower data quality (Fig. 4), meant that it was not possible to confidently link these generations across the entire study area. Overall, the lengths, widths and sinuosities of the tunnel valleys do not appear to vary significantly between generations.

However, the average directionality of the buried tunnel valleys does change between generations, as highlighted in Figure 12a. Within all four AOI, the tunnel valleys display a wide variation of directionality between generations, sometimes varying significantly from one set of valleys to the next. For example, in AOI 1, generations 1 and 2 trend NE-SW, while generations 3, 4 and 5 trend NW-SE (Fig. 12a). In general, the first two, oldest, generations in each AOI appear to follow a relatively similar trend (NE-SW for AOI 1, 2, and 4; NW-SE for AOI 3), and then directionality changes at Generation 3 (in AOI 1, 2 and 3). In AOI 4,

there is a significant change in directionality between generations 4 and 5, as in AOI 2 and AOI 3.

Clear differences in tunnel-valley orientation are also apparent across the central and northern North Sea (Fig. 12a). For example, the oldest two generations of tunnel valleys (generations 1 and 2; light and dark blue, respectively, in Fig. 12a) in the southernmost study area (AOI 1) trend approximately NE-SW, whereas in the northernmost AOI 3 the oldest two generations trend ESE-WNW and E-W. Similarly, the tunnel-valley orientation of generations 4 and 5 (orange and pink, respectively, in Fig. 12a) is strikingly different between the south (AOI 1, where they trend SE-NW) and the north (AOI 3, where they trend NNW-SSE and NE-SW). In AOI 2, the majority of tunnel valleys, which were mostly not able to be sorted into generations, display a strong NE-SW trend (Fig. 6c), apparently related to the margin of the Norwegian Channel (Figs. 4 and 6b). In AOI 3, two large tunnel valleys show a strong N-S directionality, as do others nearby but outside of the AOI (Fig. 4). AOI 4 tunnel valleys show a wide variety of directionality and a higher number of generations (Fig. 8); this complexity may reflect the higher density of tunnel valleys in this area (Fig. 10 and Section 5.3 below).

5.2 Tunnel-valley geometry - length

Around 84% of the tunnel valleys mapped from 3D seismic and magnetic data are less than 20 km in length, and around 15% of the tunnel valleys are between 20 and 100 km long (Fig. 11), although many are observed to extend out with data limits, which affects overall summaries of tunnel-valley lengths. Five of the tunnel valleys have lengths of greater than 100 km; three examples of these tunnel valleys are highlighted in Figure 11a. These three valleys trend approximately S-N or SSE-NNW from 56°N to 58°N, and have a curved geometry that is convex to the west. Tunnel valley b extends into AOI 1 where it is interpreted as part of Generation 5, the youngest set of tunnel valleys in the AOI (Fig. 5). Tunnel valley ‘a’ (Fig. 11) can also be interpreted to extend into AOI 1 (red dashed lines), which would further increase its reported length and permit its classification as Generation 5. The directionality of these long valleys is markedly different to those of the older generation 1 and 2 valleys in AOI 1, which generally trend NE-SW (Fig. 5c). We note that our measurements of tunnel-valley length are probably minimum estimates; many tunnel valleys extend beyond the data coverage, and areas of poor data quality (yellow outlines in Fig. 4) within the 3D merged datasets may preclude the correlation of valleys between parts of this study (Figs. 4 and 10).

The extreme length of the longest tunnel valleys reported in this study (Fig. 11) emphasizes their role in ice-sheet drainage and subsequent importance in the glacial and subglacial landscape. The formation of such large valleys clearly requires a significant amount of water to reach the ice-sheet bed. We find that the geometry of these large tunnel valleys adds to the body of evidence that the North Sea and northwest European tunnel valleys generally formed in stages over time rather than catastrophically (Kristensen and Huuse, 2012; Stewart et al., 2013).

5.3 Tunnel-valley density and distribution

The geological setting and glacial history of the North Sea Basin has clearly been conducive to the formation and preservation of thousands of tunnel valleys, particularly over the past *c.* 1 Ma since the basin became infilled (Ottesen et al., 2018). This study finds that tunnel valleys are also present in the northern part of the North Sea above 61°N, less than 100 km from the present-day shelf edge (Figs. 4 and 10). The highest density of tunnel valleys within the study area, as observed from both the seismic and magnetic datasets (Fig. 10a), generally corresponds to the central, deepest part of the Quaternary North Sea Basin that contains the thickest Quaternary sediments (Fig. 10b) (Ottesen et al., 2014). This finding agrees with previous works that have found that tunnel-valley density typically increases where sediment thickness is greater (Stackebrandt, 2009; Stewart et al., 2013), but may also be a consequence of greater preservation potential in areas of thicker sediment.

Here we find that, although tunnel-valley density generally correlates to Quaternary sediment thickness, the areas of highest tunnel-valley density are located slightly to the north of the thickest Quaternary sediments, at around 59°N (Fig. 10). This is partly related to data availability; for example, relatively isolated 3D seismic datasets increase density measurements around the areas marked ‘A’ and ‘B’ in Fig. 10. The high density of tunnel valleys at around 59°N (Fig. 10a) could relate to the overall glacial history of the central and northern North Sea, which has been interpreted to have had a longer history of coverage by grounded ice compared with the southern North Sea (Buckley, 2016; Ottesen et al., 2018; Rea et al., 2018).

An exception to the generally high density of tunnel valleys across the North Sea is in the Norwegian Channel (Figs. 4 and 10). Although tunnel valleys are mapped at the western margin of the Norwegian Channel, we do not identify any tunnel valleys within the channel itself. This could be because the Norwegian Channel has experienced extensive erosion during the full-glacial periods of the Mid- to Late Pleistocene, which removed evidence of

older tunnel valleys, and/or because few tunnel valleys were formed beneath the Norwegian Channel Ice Stream, during periods of ice breakup or deglaciation, while it acted as a major drainage channel to the north. The presence of numerous ENE-WSW trending valleys in AOI 2 (Fig. 6b) and nearby (Fig. 4) provides some evidence for potential meltwater drainage by tunnel valleys towards the Norwegian Channel in this scenario.

5.4 Tunnel valleys and ice sheets

During the Mid- to Late Pleistocene, at least during the Weichselian (MIS 5d - 2), Saalian (MIS ?10 - 6), and Elsterian (MIS 12) glaciations, ice sheets from the UK and Norwegian land masses coalesced and covered the North Sea Plateau at least as far south as the North Sea between Britain and the Netherlands/Denmark (Ehlers et al., 2011; Hughes and Gibbard, 2018; Lang et al., 2018). To the north, the ice-sheet margin reached the shelf edge beyond Norway and Scotland (Sejrup et al., 2005, 2016; Bradwell et al., 2008; van der Vegt et al., 2012). Figure 12 shows the maximum extent of these glaciations based on the recent compilation of Batchelor et al. (2019).

Previous studies partly constrain most reported buried tunnel valleys in the central and northern North Sea as being younger than the Brunhes-Matuyama reversal event at 780 ka and older than the LGM at 22.7 – 19.2 ka (Sejrup et al., 1994; Stewart and Lonergan, 2011; Stewart et al. 2013). Thus, the distribution and relative ages (or generations) of the tunnel valleys examined in this study may provide further insight into pre-LGM conditions in the North Sea. Compared to LGM models of ice-sheet advance and decay (Boulton and Hagdorn, 2006; Clark et al., 2012; Hughes and Gibbard, 2018), some of the observed tunnel-valley generational trends can be accounted for if the evolution of the older ice sheets behaved in a similar way to those modelled for the LGM, and if the tunnel valleys are considered to drain roughly towards a relatively stable ice margin during ice-sheet breakup and/or retreat.

For example, the large complex of Generation 5 (youngest) anastomosing tunnel valleys observed in AOI 1 could have formed in relation to a large southern lobe of the British and Irish Ice Sheet (BIIS) retreating to the northwest towards the British mainland, as indicated in Clark et al.'s (2012) model of asymmetric post-LGM breakup. N-S and NNE-SSW trending tunnel valleys in AOI 3 and AOI 4 may relate to a similar scenario as that presented by Bradwell et al. (2008) or Graham et al. (2011), whereby the northern part of the LGM BIIS ice-sheet is influenced by a marine incursion from the north during breakup, resulting in an E-W trending ice margin and northwards drainage of meltwater by tunnel valleys.

Other patterns within the tunnel-valley generations are more difficult to explain. For example, the two oldest generations of tunnel valleys within AOI 1 trend in the opposite direction (NE-SW) to those described above; perhaps relating to a NE-retreating lobe of the Scandinavian Ice Sheet (SIS). Similarly, the concave-west curving geometry of the very large tunnel valleys observed in Figure 11 would, especially if considered part of the Generation 5 set of tunnel valleys observed in AOI 1, be difficult to reconcile with the northwest-retreating lobe considered above.

In AOI 2 at least, the influence of the western margin of the Norwegian Channel appears to be fairly significant to tunnel-valley formation across a number of generations (Fig. 6). The Norwegian Channel Ice Stream is suggested to have collapsed and retreated rapidly from the shelf break along the Norwegian Channel following the LGM (Clark et al., 2012; Sejrup et al., 2016). Early deglaciation of the Norwegian Channel during earlier glacial periods would also presumably isolate the retreating SIS from the BIIS over the North Sea Plateau.

One scenario which may account for some of the observed variation in tunnel-valley orientation is presented in Figure 12. In this hypothesis, ice sheets which previously coalesced across the North Sea are influenced during deglaciation or ice-sheet retreat by the collapse, or 'switching off', of ice streaming along the Norwegian Channel, which effectively separates the BIIS and SIS. An ice dome remains within the North Sea, down-wasting and producing a set of tunnel valleys draining towards its edges, with variable tunnel-valley directionality depending on the shape of the down-wasting ice. Subglacial drainage patterns, and therefore tunnel valleys, could, for example, reflect the shifting position of such an ice divide or ice dome over the North Sea Plateau between successive deglaciations, which would route water in different directions depending on the local morphology of the ice-sheet surface and its internal dynamics. It is worth noting that, even in this scenario, AOI 4 is hundreds of kilometres from any potential ice margins; the variability of the observed dense tunnel valleys in this area may be entirely related to local controls on ice thickness and dynamics.
Without being able to conclusively link the tunnel-valley generations across the study area, and without absolute ages for the tunnel valleys, correlating the tunnel-valley generations to potential Quaternary ice-sheet configurations remains difficult. Given that the tunnel valleys were largely formed within thick, unconsolidated sediments, without structural or bedrock control, the main conclusion of this study is that the changing orientations and geometries of the tunnel valleys across the four AOI, and between generations, shows that the dynamics of

the ice sheets under which the tunnel valleys formed must have been significantly different between episodes of formation.

To advance further in our understanding of the formation and geometry of tunnel valleys requires higher-resolution seismic data and the acquisition of material for dating. Although high-resolution site survey data are available to better image offshore tunnel-valley fill, these types of surveys are generally only collected over small areas (up to several km^2) and it is difficult to extrapolate interpretations from such data across networks of tunnel valleys that stretch for tens to hundreds of kilometres.

6. CONCLUSIONS

- We use a combination of 3D seismic data and airborne magnetic data to map, for the first time, the distribution of more than 2200 tunnel valleys in the British and Norwegian sectors of the central and northern North Sea. We find a strong correlation between the location of tunnel valleys derived from magnetic data and 3D seismic cubes.
- Our broad data coverage permits the identification of several tunnel valleys of extreme length. The longest tunnel valley is 155 km long, and several other valleys have lengths of > 80 km. The significant amount of water required to excavate and fill these valleys adds to the body of evidence that tunnel valleys generally form in stages over time rather than catastrophically.
- Tunnel valleys are mapped at the western margin of the Norwegian Channel yet are not identified within the channel itself. It is possible that tunnel valleys were not formed within the Norwegian Channel because of early rapid deglaciation of the Norwegian Channel Ice Stream following glacial maxima. Evidence for tunnel valleys may also have been removed from the Norwegian Channel by extensive ice-stream erosion during the Mid- to Late Pleistocene.
- To the west of the Norwegian Channel, the down-wasting of an ice cap centred over the North Sea Plateau could explain the high density and variable orientation of tunnel valleys in the central and northern North Sea, as well as the pattern of subglacial drainage towards the Norwegian Channel that is suggested by the orientation of some of the valleys.

- The highest density of tunnel valleys generally corresponds to the central, deepest part of the Quaternary North Sea Basin, suggesting a link between sediment thickness and the formation and/or preservation of tunnel valleys.
- Five generations of tunnel valleys are reported from three AOI in the central and northern North Sea, whilst seven generations are interpreted from a fourth AOI. Tunnel-valley orientation is shown to vary significantly between generations, suggesting that subglacial meltwater followed a different drainage pattern between ice-retreat events.

ACKNOWLEDGEMENTS

We acknowledge AkerBP for permission to use their seismic database and workspace to carry out the seismic work in this study. We thank TGS for permission to use their magnetic data and to present a regional 2D seismic line. We also thank PGS for permission to publish data from the PGS Megasurvey and Searcher Seismic for access to the Utstord 3D seismic cube. CLB was in receipt of a Norwegian VISTA post-doctoral scholarship during this work. Schlumberger is thanked for access to the Petrel software. We thank Jutta Winsemann and two anonymous reviewers for their helpful reviews of this work.

REFERENCES

Batchelor, C.L., Ottesen, D., Dowdeswell, J.A., 2017. Quaternary evolution of the northern North Sea margin through glacigenic debris-flow and contourite deposition. J. Quat. Sci. 32, 416–426.

Batchelor, C.L., Margold, M., Krapp, M., Murton, D.K., Dalton, A.S., Gibbard, P.L., Stokes, C.R., Murton, J.B., Manica, A., 2019. The configuration of Northern Hemisphere ice sheets through the Quaternary. Nat. Comm. 10(1), 1–10.

Benn, D. I., Evans, D. J. A., 2010. Glaciers and Glaciations. Arnold, London.

Benvenuti, A., Šegvić, B., Moscariello, A., 2018. Tunnel valley deposits from the southern North Sea–material provenance and depositional processes. Boreas 47(2), 625–642.

Boulton, G., Hindmarsh, R.C.A., 1987. Sediment deformation beneath glaciers: rheology and geological consequences. J. Geophys. Res. 92, 9059–9082.

Boulton, G., Hagdorn, M., 2006. Glaciology of the British Isles Ice Sheet during the last glacial cycle: form, flow, streams and lobes. Quat. Sci. Rev. 25(23-24), 3359–3390.

Boulton, G., Hagdorn, M., Maillot, P.B., Zatsepin, S., 2009. Drainage beneath ice sheets: groundwater-channel coupling and the origin of esker systems: part II – theory and simulations of a modern system. Quat. Sci. Rev. 28, 621–638.

Bradwell, T., Stoker, M.S., Golledge, N.R., Wilson, C.K., Merritt, J.W., Long, D., Everest, J.D., Hestvik, O.B., Stevenson, A.G., Hubbard, A.L., Finlayson, A.G., 2008. The northern sector of the last British Ice Sheet: maximum extent and demise. Earth-Sci. Rev. 88, 207-226.

Brahimi, S., Le Maire, P., Ghienne, J.M., Munschy, M., 2019. Deciphering channel networks from aeromagnetic potential field data: the case of the North Sea Quaternary tunnel valleys. Geophys. J. Int. 220, 1447–1462. Doi: 10.1093/gji/ggz494

Buckley, F.A., 2016. A glaciogenic sequence from the Early Pleistocene of the Central North Sea. J. Quat. Sci. Doi:10.1002/jqs.2867.

Clark, C.D., Hughes, A.L., Greenwood, S.L., Jordan, C., Sejrup, H.P., 2012. Pattern and timing of retreat of the last British-Irish Ice Sheet. Quat. Sci. Rev. 44, 112-146.

Coughlan, M., Fleischer, M., Wheeler, A. J., Hepp, D. A., Hebbeln, D., Mörz, T., 2018. A revised stratigraphical framework for the Quaternary deposits of the German North Sea sector: a geological-geotechnical approach. Boreas 47, 80-105.

Dowdeswell, J.A., Ottesen, D., 2013. Buried iceberg ploughmarks in the early Quaternary sediments of the central North Sea: a two-million-year record of glacial influence from 3D seismic data. Mar. Geol. 344, 1–9.

Ehlers, J., Linke, G., 1989. The origin of deep buried channels of Elsterian age in northwest Germany. J. Quat. Sci. 4, 255 –265.

Ehlers, J., Grube, A., Stephan, H.J., Wansa, S., 2011. Pleistocene glaciations of northern Germany – new results. In: Ehlers, J., Gibbard, P.L., Huhges, P.D. (Eds.). Quaternary Glaciations – Extent and Chronology – a closer look. Developments in Quaternary Science 15. Elsevier, Amsterdam, 149–162.

Fichler, C., Henriksen, S., Rueslåtten, H., Hovland, M., 2005. North Sea Quaternary morphology from seismic and magnetic data: indications for gas hydrates during glaciation? Pet. Geosci. 11, 331–337.

Gatliff, R.W., Richards, P.C., Smith, K., Graham, C.C, McCormack, M., Smith, N.J.P., Long, D., Cameron, T.D.J., Evans, D., Stevenson, A.G., Bulat, J., Ritchie, J.D., 1994. United Kingdom offshore regional report: the geology of the central North Sea. HMSO for the British Geological Survey, London.

Gibbard, P.L., 1988. The history of the great northwest European rivers during the past three million years. Phil. Trans. Royal Soc. London, Series B, 318, 559–602.

Graham, A.G.C., 2007. Reconstructing Pleistocene Glacial Environments in the Central North Sea Using 3D Seismic and Borehole Data. PhD thesis: University of London, 410 pp.

Graham, A.G.C., Lonergan, L., Stoker, M.S., 2010. Depositional environments and chronology of Late Weichselian glaciation and deglaciation in the central North Sea. Boreas, 39(3), 471-491.

Graham, A.G.C., Stoker, M.S., Lonergan, L., Bradwell, T., Stewart, M.A., 2011. The Pleistocene glaciations of the North Sea basin. In: Developments in Quaternary Sciences 15, 261-278. Elsevier.

Hepp, D.A., Hebbeln, D., Kreiter, S., Keil, H., Bathmann, C., Ehlers, J., Mörz, T., 2012. An east-west-trending Quaternary tunnel valley in the south-eastern North Sea and its seismic-sedimentological interpretation. J. Quat. Sci. 27, 844-853.

Hughes, P., Gibbard, P.L., 2018. Global glacier dynamics during 100 ka Pleistocene glacial cycles. Quat. Res., 1-22. Doi: 10.1017/qua.2018.37.

Huuse, M., Lykke-Andersen, H., 2000. Overdeepened Quaternary valleys in the eastern Danish North Sea: morphology and origin. Quat. Sci. Rev. 19, 1233–1253.

Johnson, H., Richards, P.C., Long, D., Graham, C.C., 1993. United Kingdom Offshore Regional Report: The Geology of the northern North Sea. HMSO for the British Geological Survey, London.

Kehew, A.E., Piotrowski, J.A., Jørgensen, F., 2012. Tunnel valleys: Concepts and controversies – A Review. Earth-Sci. Rev. 113, 33–58.

Kluiving, S.J., Bosch, J.H.A., Ebbing, J.H.J., Mesdag, C.S., Westerhoff, R.S., 2003. Onshore and offshore seismic and lithostratigraphic analysis of a deeply incised Quaternary buried valley-system in the Northern Netherlands. J. Appl. Geophys. 53, 249–271.

Kristensen, T.B., Huuse, M., 2012. Multistage erosion and infill of buried Pleistocene tunnel valleys and associated seismic velocity effects. In: Huuse, M., Redfern, J., Le Heron, D.P., Dixon, R.J., Moscariello, A., Craig, J. (Eds.), Glaciogenic Reservoirs and Hydrocarbon Systems. Geol. Soc., London, Spec. Publ. 368, 159–172.

Kristensen, T.B., Huuse, M., Piotrowski, J.A., Clausen, O.R., 2007. A morphometric analysis of tunnel valleys in the eastern North Sea based on 3D seismic data. J. Quat. Sci. 22, 801–815.

Kvamme, K.L., 2003. Geophysical surveys as landscape archaeology. Amer. Antiquity 68, 435–457.

Laban, C., van der Meer, J.J.M., 2011. Pleistocene glaciation in the Netherlands. In: Ehlers, J., Gibbard, P.L., Hughes, P.D. (Eds.), Quaternary Glaciations – Extent and Chronology, a Closer Look, 247-260. Elsevier, Amsterdam.

Lamb, R.M., Huuse, M., Stewart, M.A., 2016. Early Quaternary sedimentary processes and palaeoenvironments in the central North Sea. J. Quat. Sci. 32, 127–144.

Lamb, R.M., Harding, R., Huuse, M., Stewart, M.A., Brocklehurst, S.H., 2017. The early Quaternary North Sea Basin. J. Geol. Soc. 175, 275–290.

Lang, J., Lauer, T., Winsemann, J., 2018. New age constraints for the Saalian glaciation in northern central Europe: Implications for the extent of ice sheets and related proglacial lake systems. Quat. Sci. Rev. 180, 240–259.

Lee, J.R., Busschers, F.S., Sejrup, H.P., 2012. Pre-Weichselian Quaternary glaciations of the British Isles, The Netherlands, Norway and adjacent marine areas south of 68°N: implications for long-term ice sheet development in northern Europe. Quat. Sci. Rev. 44, 213-228.

Lelandais, T., Mourgues, R., Ravier, É., Pochat, S., Strzerzynski, P. and Bourgeois, O., 2016. Experimental modeling of pressurized subglacial water flow: Implications for tunnel valley formation. J. Geophys. Res.: Earth Surf. 121, 2022-2041.

Livingstone, S.J., Clark, C.D., 2016. Morphological properties of tunnel valleys of the southern sector of the Laurentide Ice Sheet and implications for their formation. Earth Surf. Dynam. 4, 567-589.

Lonergan, L., Maidment, S.C.R., Collier, J.S., 2006. Pleistocene subglacial tunnel valleys in the central North Sea basin: 3-D morphology and evolution. J. Quat. Sci. 21, 891–903.

Lutz, R., Kalka, S., Gaedicke, C., Reinhardt, L., Winsemann, J., 2009. Pleistocene tunnel valleys in the German North Sea: spatial distribution and morphology. Zeitschrift der Deutschen Gesellschaft für Geowissenschaften 160, 225–235.

Montelli, A., Dowdeswell, J.A., Pirogova, A., Terekhina, Y., Tokarev, M., Rybin, N., Martyn, A., Khoshtariya, V., 2020. Deep and extensive meltwater system beneath the fromer Eurasian Ice Sheet in the Kara Sea. Geology 48, doi.org/10.1130/G46968.1.

Moreau, J., Huuse, M., 2014. Infill of tunnel valleys associated with landward-flowing ice sheets. G3: Geochem., Geophys., Geosyst. 15, doi: 10.1002/2013/2013GC005007.

Moreau, J., Huuse, M., Janszen, A., van der Vegt, P., Gibbard, P.L., Moscariello, A., 2012. The glaciogenic unconformity of the southern North Sea. In: Huuse, M., Redfern, J., Le Heron, D. P., Dixon, R. J., Moscariello, A., Craig, J. (Eds.), Glaciogenic Reservoirs and Hydrocarbon Systems. Geol. Soc., London, Spec. Publ. 368.

Muther, D., Back, S., Reuning, L., Kukla, P., Lehmkuhl, F., 2012. Middle Pleistocene landforms in the Danish Sector of the southern North Sea imaged on 3D seismic data. In: Huuse, M., Redfern, J., Le Heron, D. P., Dixon, R. J., Moscariello, A., Craig, J. (Eds.), Glaciogenic Reservoirs and Hydrocarbon Systems. Geol. Soc., London, Spec. Publ. 368, 111–127.

O´ Cofaigh, C., 1996. Tunnel valley genesis. Progr. in Phys. Geogr. 20, 1– 19.

Olesen, O., Brönner, M., Ebbing, J., Gellein, J., Gernigon, L., Koziel, J., Lauritsen, T., Myklebust, R., Pascal, C., Sand, M., Solheim, D., Usov, S., 2010. New aeromagnetic and gravity compilations from Norway and adjacent areas: methods and applications. In: Geol. Soc., London, Pet. Geol. Conf. ser. (Vol. 7, No. 1, 559-586). Geol. Soc. London, doi: https://doi.org/10.1144/0070559

Olesen, O., Brönner, M., Ebbing, J., Elvebakk, H., Gellein, J., Koziel, J., Lauritsen, T., Lutro, O., Maystrenko, Y., Müller, C., Nasuti, A., Osmundsen, P.T., Slagstad, T., Storrø, G., 2013. Coop Phase I - Crustal Onshore-Offshore Project. NGU-report 2013.002, 359pp.

Ottesen, D., Dowdeswell, J.A., Bugge, T., 2014. Morphology, sedimentary infill and depositional environments of the Early Quaternary North Sea Basin (56-62°N). Mar. Pet. Geol. 56, 123–146.

Ottesen, D., Stokes, C.R., Bøe, R., Rise, L., Longva, O., Thorsnes, T., Olesen, O., Bugge, T., Lepland, A., Hestvik, O.B., 2016. Landform assemblages and sedimentary processes along the Norwegian Channel Ice Stream. Sedim. Geol. 338, 115-137.

Ottesen, D., Batchelor, C.L., Dowdeswell, J.A., Løseth, H., 2018. Morphology and pattern of Quaternary sedimentation in the North Sea Basin (52-62ºN). Mar. Pet. Geol. 98, 836–859.

Overeem, I., Weltje, G.J., Bishop-Kay, C., Kroonenberg, S.B., 2001. The Late Cenozoic Eridanos delta system in the Southern North Sea Basin: a climate signal in sediment supply? Basin Res. 13, 293–312.

Piotrowski, J.A., 1997. Subglacial hydrogeology in northwestern Germany during the last glaciation: groundwater flow, tunnel valleys and hydrogeological cycles. Quat. Sci. Rev. 16, 169–185.

Praeg, D., 2003. Seismic imaging of mid-Pleistocene tunnel-valleys in the North Sea Basin – high resolution from low frequencies. J. Applied Geophys. 53, 273–298.

Rea, B.R., Newton, A.M.W., Lamb, R.M., Harding, R., Bigg, G.R., Rose, P., Spagnolo, M., Huuse, M., Cater, J.M.L., Archer, S., Buckley, F., Halliyeva, M., Huuse, J., Cornwell, D.G., Brocklehurst, S.H., Howell, J.A., 2018. Extensive marine-terminating ice sheets in Europe from 2.5 million years ago. Science Advances 4, eaar8327.

Reinardy, B.T., Hjelstuen, B.O., Sejrup, H.P., Augedal, H., Jørstad, A., 2017. Late Pliocene-Pleistocene environments and glacial history of the northern North Sea. Quat. Sci. Rev. 158, 107-126.

Rose, P., Byerley, G., Vaughan, O., Cater, J., Rea, B.R., 2016. Aviat: a Lower Pleistocene shallow gas hazard developed as a fuel gas supply for the Forties Field. In: Bowman, M., Levell, B. (Eds.), Petroleum Geology of NW Europe: 50 Years of Learning. Proceedings of the 8th Petroleum Geology Conference. Geol. Soc. London.

Roskosch, J. Winsemann, J., Polom, U., Brandes, C., Tsukamoto, S., Weitkamp, A., Bartholomäus, W.A., Henningsen, D., Frechen, M., 2015. Luminescence dating of ice-marginal deposits in northern Germany: evidence for repeated glaciations during the Middle Pleistocene (MIS 12 to MIS 6). Boreas 44, 103-126.

Sandersen, P.B.E., Jørgensen, F., 2012. Substratum control on tunnel-valley formation in Denmark. In: Huuse, M., Redfern, J., Le Heron, D.P., Dixon, R.J., Moscariello, A., Craig, J. (Eds.), Glaciogenic Reservoirs and Hydrocarbon Systems. Geol. Soc., London, Spec. Publ. 368, 145–157.

Sejrup, H.P., Haflidason, H., Aarseth, I., King, E., Forsberg, C.F., Long, D., Rokoengen, K., 1994. Late Weichselian glaciation history of the northern North Sea. Boreas 23(1), 1-13.

Sejrup, H.P., Aarseth, I., Haflidason, H., Løvlie, R., Bratten, Å., Tjøstheim, G., Forsberg, C.F., Ellingsen, K.L., 1995. Quaternary of the Norwegian Channel: glaciation history and palaeoceanography. Norw. J. Geol. 75, 65–87.

Sejrup, H.P., Hjelstuen, B.O., Dahlgren, K.T., Haflidason, H., Kuijpers, A., Nygård, A., Praeg, D., Stoker, M.S., Vorren, T.O., 2005. Pleistocene glacial history of the NW European continental margin. Mar. Pet. Geol. 22, 1111–1129.

Sejrup, H.P., Clark, C.D., Hjelstuen, B.O., 2016. Rapid ice sheet retreat triggered by ice stream debuttressing: Evidence from the North Sea. Geology 44, 355–358.

Shaw, J., Gilbert, R., 1990. Evidence for large-scale subglacial meltwater flood events in southern Ontario and northern New York State. Geology 18, 1169–1172.

Stackebrandt, W., 2009. Subglacial channels of Northern Germany – a brief review. Zeitschrift der Deutschen Gesellschaft für Geowissenschaften 160, 203–210.

Stewart, M.A., Lonergan, L., 2011. Seven glacial cycles in the middle–late Pleistocene of northwest Europe: Geomorphic evidence from buried tunnel valleys. Geology 39, 283–286.

Stewart, M.A., Lonergan, L., Hampson, G., 2012. 3D seismic analysis of buried tunnel valleys in the Central North Sea: tunnel valley fill sedimentary architecture. In: Huuse, M., Redfern, J., Le Heron, D.P., Dixon, R.J., Moscariello, A., Craig, J. (Eds.), Glaciogenic Reservoirs and Hydrocarbon Systems. Geol. Soc., London, Spec. Publ. 368, 173–184.

Stewart, M.A., Lonergan, L., Hampson, G., 2013. 3D seismic analysis of buried tunnel valleys in the central North Sea: morphology, cross-cutting generations and glacial history. Quat. Sci. Rev. 72, 1–17.

Stewart, M.A., 2016. Assemblage of buried and seabed tunnel valleys in the central North Sea: from morphology to ice-sheet dynamics. In: Dowdeswell, J.A., Canals, M., Jakobsson, M., Todd, B.J., Dowdeswell, E.K., Hogan, K.A. (Eds.), Atlas of Submarine Glacial Landforms: Modern, Quaternary and Ancient. Geol. Soc. London Mem. 46, 317–320.

Stoker, M.S., 1987. Lower Pleistocene deltaic and marine sediments in boreholes from the central North Sea. J. Quat. Sci. 2, 87–96.

Stoker, M.S., Skinner, A., Fyfe, J.A., Long, D., 1983. Paleomagnetic evidence for Early Pleistocene in the central and northern North Sea. Nature 304, 332-334.

Stuart, J.Y., Huuse, M., 2012. 3D seismic geomorphology of a large Plio-Pleistocene delta – bright spots and contourites in the Southern North Sea. Mar. Pet. Geol. 38, 85–93.

Thöle, H., Gaedicke, C., Kuhlmann, G., Reinhardt, L., 2014. Late Cenozoic sedimentary evolution of the German North Sea – A seismic stratigraphic approach. Newsl. on Strat. 47, 299–329.

Toucanne, S., Zaragosi, S., Bourillet, J.F., Cremer, M., Eynaud, F., Vliet-Lanoe, Van, Penaud, A., Fontanier, C., Turon, J.L., Cortijo, E., Gibbard, P.L., 2009. Timing of massive 'Fleuve Manche' discharges over the last 350kyr: insights into the European ice-sheet oscillations and the European drainage network from MIS 10 to 2. Quat. Sci. Rev. 28, 1238–1256.

van der Vegt, P., Janszen, A., Moscariallo, A., 2012. Tunnel valleys: Current knowledge and future perspectives. In: Huuse, M., Redfern, J., Le Heron, D.P., Dixon, R.J., Moscariello, A., Craig, J. (Eds.), Glaciogenic Reservoirs and Hydrocarbon Systems. Geol. Soc. London Spec. Publ. 368, 75–97.

Wingfield, R.T.R., 1989. Glacial incisions indicating middle and upper Pleistocene ice limits off Britain. Terra Nova 1, 538–548.

Wingfield, R.T.R., 1990. The origin of major incisions within the Pleistocene deposits of the North Sea. Mar. Geol. 91, 31–52.

Winsemann, J., Koopmann, H., Tanner, D.C., Lutz, R., Lang, J., Brandes, C., Gaedicke, C., 2020. Seismic interpretation and structural restoration of the Heligoland glaciotectonic thrust-fault complex: Implications for multiple deformation during (pre-) Elsterian to Warthian ice advances into the southern North Sea Basin. Quat. Sci. Rev. 227, p.106068.

Wright, H.E., 1973. Tunnel valleys, glacial surges and subglacial hydrology of the Superior Lobe, Minnesota. In: Black, R.F., Goldtwait, R.P., Willman, H.B. (Eds.), The Wisconsinan Stage. Geol. Soc. Amer. Mem. 136, 251-276.

FIGURE CAPTIONS

Figure 1. Location map of the study area in the northern and central North Sea, showing the distribution of the 3D seismic data and aeromagnetic data used in this work. Dark blue lines are national boundaries. AOI = Area of interest.

Figure 2. Regional 2D seismic line across the North Sea Basin (NW-SE) showing the distribution of tunnel valleys within the Quaternary stratigraphy, provided by TGS. Image adapted from Ottesen et al. (2018) with location in Figure 1. URU = Upper Regional Unconformity. A velocity of 1800 m/s is used for depth conversion.

Figure 3. (a) Time-slice (100 ms depth) of four rectangles of the PGS Megasurvey, showing how the individual 3D seismic surveys have been merged and arranged into a regular framework. White parallel lines show the seismic line acquisition directions within the different cubes. Location is in Fig. 1. (b) Seismic profile showing the variable quality of the data within the merged 3D cubes. The profile location is shown in (a). (c) Map of the magnetic data, showing how tunnel-valley infill can be characterised by both positive (red dashed lines) and negative (blue dashed lines) magnetic anomalies.

Figure 4. The distribution of tunnel valleys in the northern and central North Sea as mapped in this study using 3D seismic data (black lines) and aeromagnetic data (red lines). Dark blue lines are national boundaries.

Figure 5. (a) Seismic time-slice through the tunnel valleys in AOI 1 is 300 ms TWT in the central North Sea. (b) Interpretation of the five generations of tunnel valleys shown in (a). (c) Rose diagrams showing the orientation of the different generations of tunnel valleys. Colours are the same as in (a) and (b). (d) Seismic profile through some of the tunnel valleys in AOI 1.

Figure 6. (a) Seismic time-slice through some of the tunnel valleys in AOI 2 at 264 ms TWT in the Norwegian sector of the central North Sea (Utstord cube). (b) Interpretation of the five generations of tunnel valleys shown in (a), together with the tunnel valleys that were not assigned a generation (grey). (c) Rose diagrams showing the orientation of the different

generations of tunnel valleys. Colours are the same as in (a) and (b). (d) Seismic profile through some of the tunnel valleys in AOI 2.

Figure 7. (a) Seismic time-slice through some of the tunnel valleys in AOI 3 in the northern North Sea at 252 ms TWT. Subtle NNW-SSE 'stripes' in the data are artefacts relating to data acquisition. (b) Interpretation of the five generations of tunnel valleys shown in (a). (c) Rose diagrams showing the orientation of the different generations of tunnel valleys. Colours are the same as in (a) and (b). (d) Seismic profile through some of the tunnel valleys in AOI 3.

Figure 8. (a) Seismic time-slice through the tunnel valleys in AOI 4 at 372 ms TWT in the British sector of the central North Sea. Subtle N-S 'stripes' in the data are artefacts relating to data acquisition. (b) Interpretation of the seven generations of tunnel valleys shown in (a). (c) Rose diagrams showing the orientation of the different generations of tunnel valleys. Colours are the same as in (a) and (b). (d) Seismic profile through some of the tunnel valleys in AOI 4.

Figure 9. Example showing the mapping of tunnel valleys using magnetic data and 3D seismic data in the central North Sea. Location is in Fig. 1. (a) Map of the magnetic data. Light blue lines show those areas that are covered by both the 3D seismic and magnetic data. (b) Interpretation of tunnel valleys from 3D seismic and magnetic data where they are both available (black lines) and from magnetic data only where 3D seismic data is absent (green lines). The overlap between the black and green lines shows the use of both magnetic and 3D seismic data to detect tunnel valleys.

Figure 10. (a) Map showing the density of tunnel valleys in the central and northern North Sea, derived from 3D seismic and aeromagnetic data. The extents of the 3D seismic and magnetic datasets are shown by the white and red lines, respectively. Dark blue lines are national boundaries. Letters A and B denote examples of regions in which the availability of 3D seismic data probably partly explains the relatively high density of tunnel valleys. (b) Map showing the thickness of Quaternary sediments in the central and northern North Sea Basin, adapted from Ottesen et al. (2014).

Figure 11. Interpretation map showing the three longest tunnel valleys, valleys a, b and c, that have been identified in the central and northern North Sea. Location is in Fig. 1. Tunnel valley b extends into AOI 1, where it was assigned to the youngest tunnel-valley generation -

Generation 5 (Fig. 5). Red dashed lines show that tunnel valley a may also extend into AOI 1. Inset shows a histogram of the length of more than 2200 tunnel valleys in the central and northern North Sea. Note the logarithmic scale of the y-axis.

Figure 12. (a) Map showing the orientation of the different generations of tunnel valleys in the four AOI in the central and northern North Sea. Also shown is the maximum extent of the European Ice Sheet during the LGM (dark blue line), MIS 6 (Saalian Glaciation; light green line), and MIS 12 (Elsterian Glaciation; orange line), derived from best-estimate reconstructions of Batchelor et al. (2019). Tentative ice-sheet configurations during the last deglaciation are shown by the dashed black lines with purple fill. Coloured arrows show tunnel-valley orientations as reported in this study. Note that the different generations of tunnel valleys are not correlated between the four AOI. Grey arrows show simplified versions of the dominant tunnel-valley orientations reported from the southern North Sea and northwest Europe as summarised by van der Vegt, (2012), and those from the German North Sea including Müther et al. (2012), Hepp et al., (2012) and Winsemann et al., (2020). Red and black outlines show the extent of the aeromagnetic and seismic data used in this study, respectively. The dark green outline is the western margin of the Norwegian Channel. (b) Profile showing the present-day topography across the central North Sea, from Scotland to southern Norway. Hypothesised ice-sheet configurations during the last deglaciation are shown by the dashed lines with purple fill.

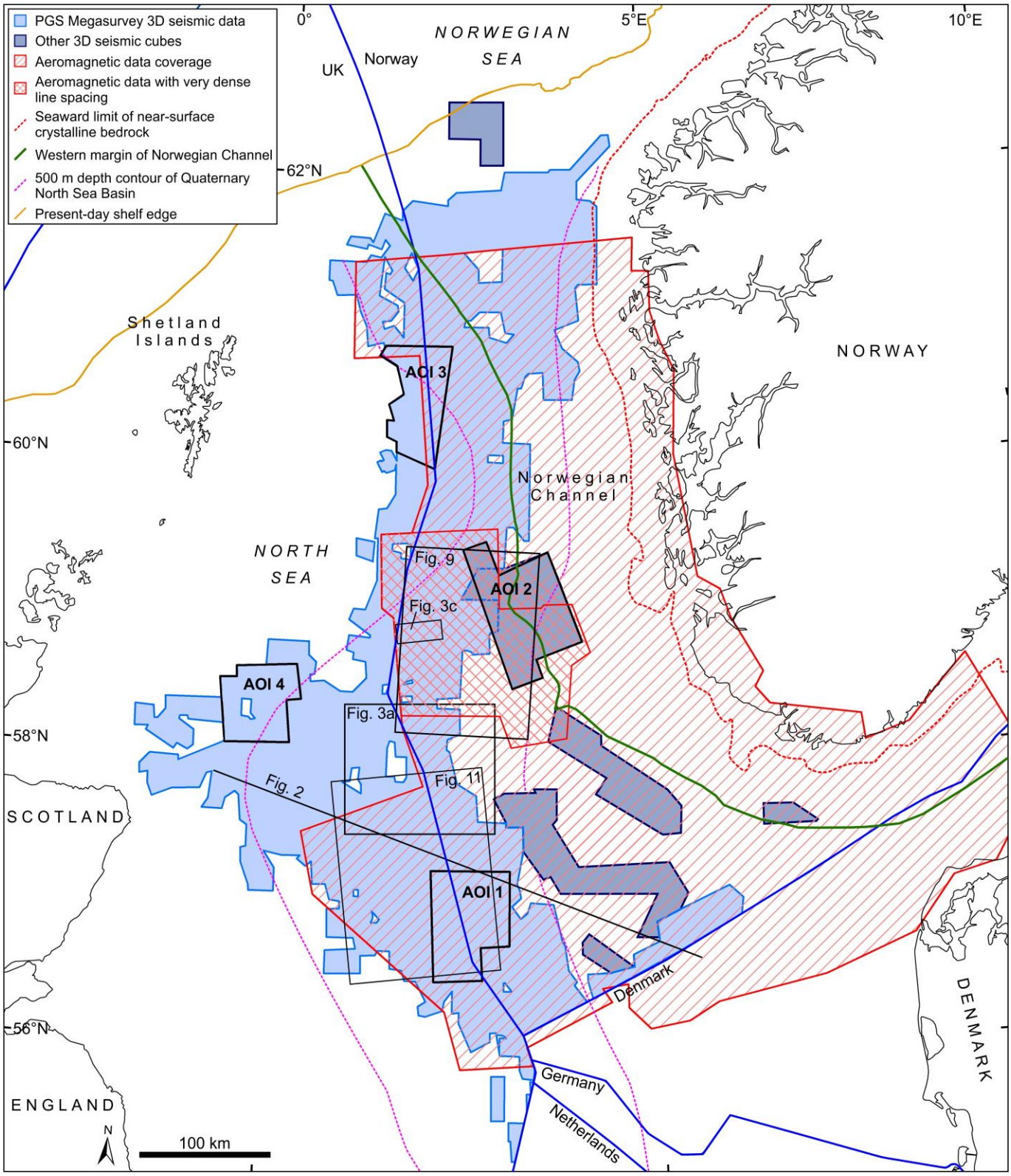
PGS Megasurvey 3D seismic data
Other 3D seismic cubes
Aeromagnetic data coverage
Aeromagnetic data with very dense line spacing
Seaward limit of near-surface crystalline bedrock
Western margin of Norwegian Channel
500 m depth contour of Quaternary North Sea Basin
Present-day shelf edge
0°
5°E
10°E
NORWEGIAN SEA
UK
Norway
62°N
Shetland Islands
NORWAY
AOI 3
60°N
Norwegian Channel
NORTH SEA
Fig. 9
AOI 2
Fig. 3c
AOI 4
Fig. 3a
58°N
Fig. 2
Fig. 11
SCOTLAND
AOI 1
Denmark
DENMARK
56°N
Germany
Netherlands
ENGLAND
N
100 km

Figure 1

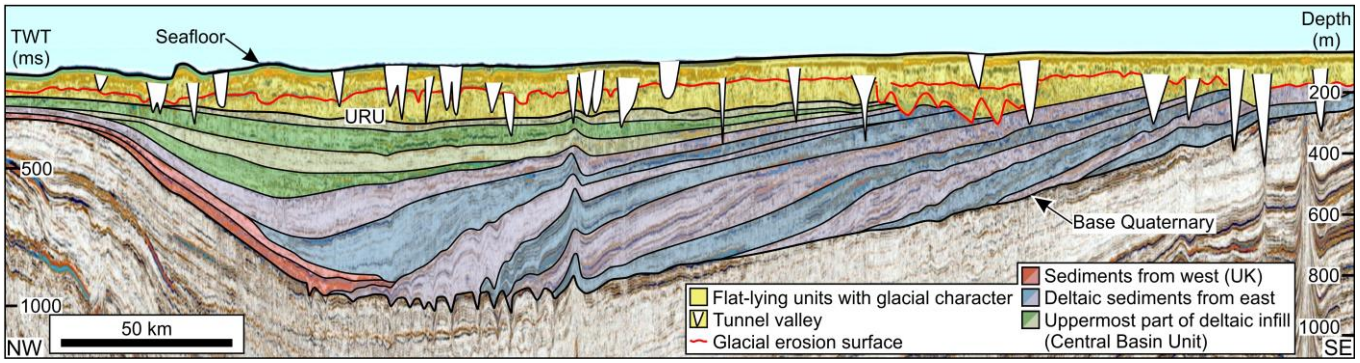
TWT
(ms)
Seafloor
URU
500
1000
50 km
NW
Depth
(m)
200
400
600
800
1000
SE
Base Quaternary
Flat-lying units with glacial character
Tunnel valley
Glacial erosion surface
Sediments from west (UK)
Deltaic sediments from east
Uppermost part of deltaic infill
(Central Basin Unit)

Figure 2

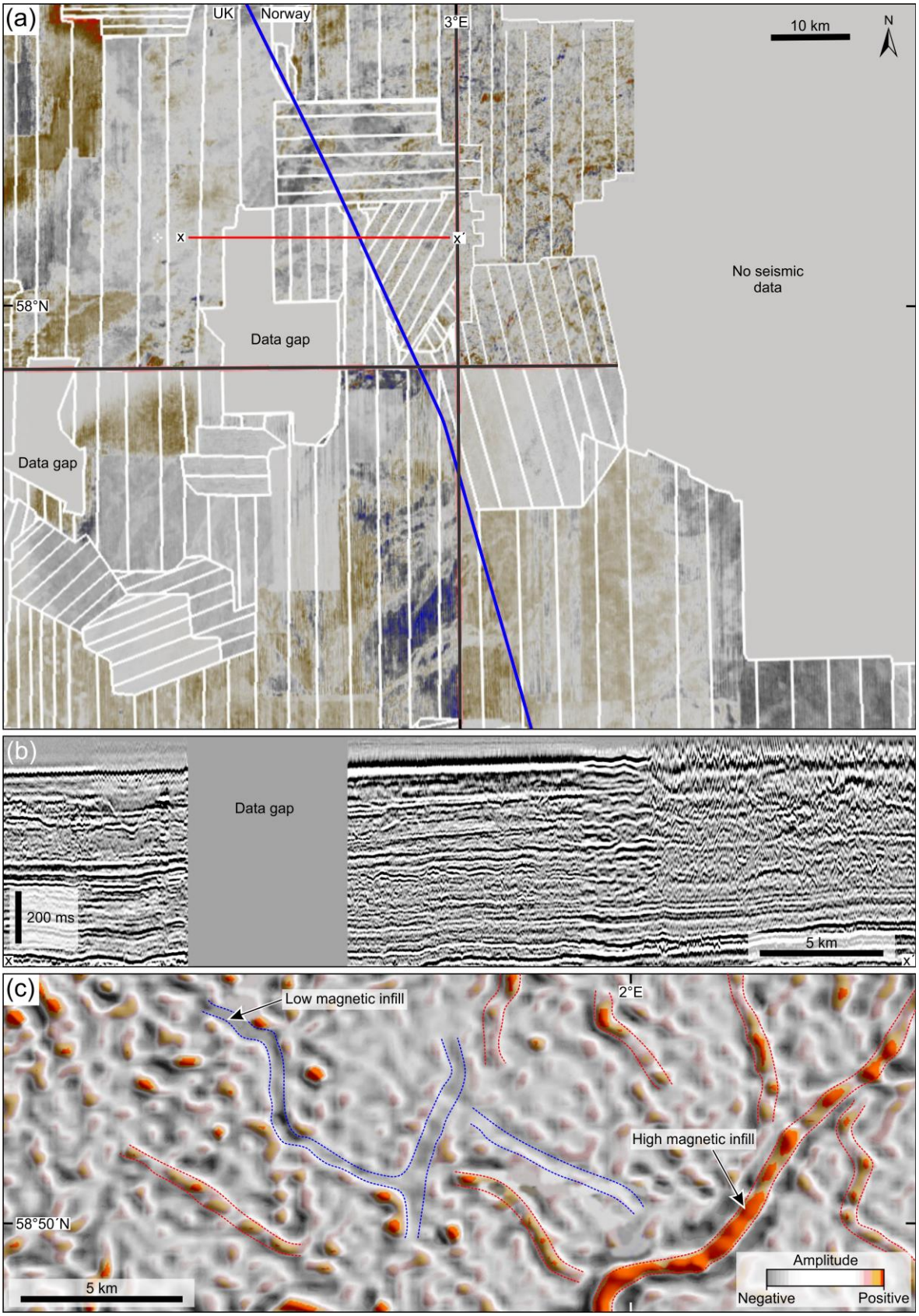
(a)
UK
Norway
3°E
10 km
N
x
x´
No seismic data
58°N
Data gap
Data gap
(b)
Data gap
200 ms
5 km
x
x´
(c)
Low magnetic infill
2°E
High magnetic infill
58°50´N
5 km
Amplitude
Negative
Positive

Figure 3

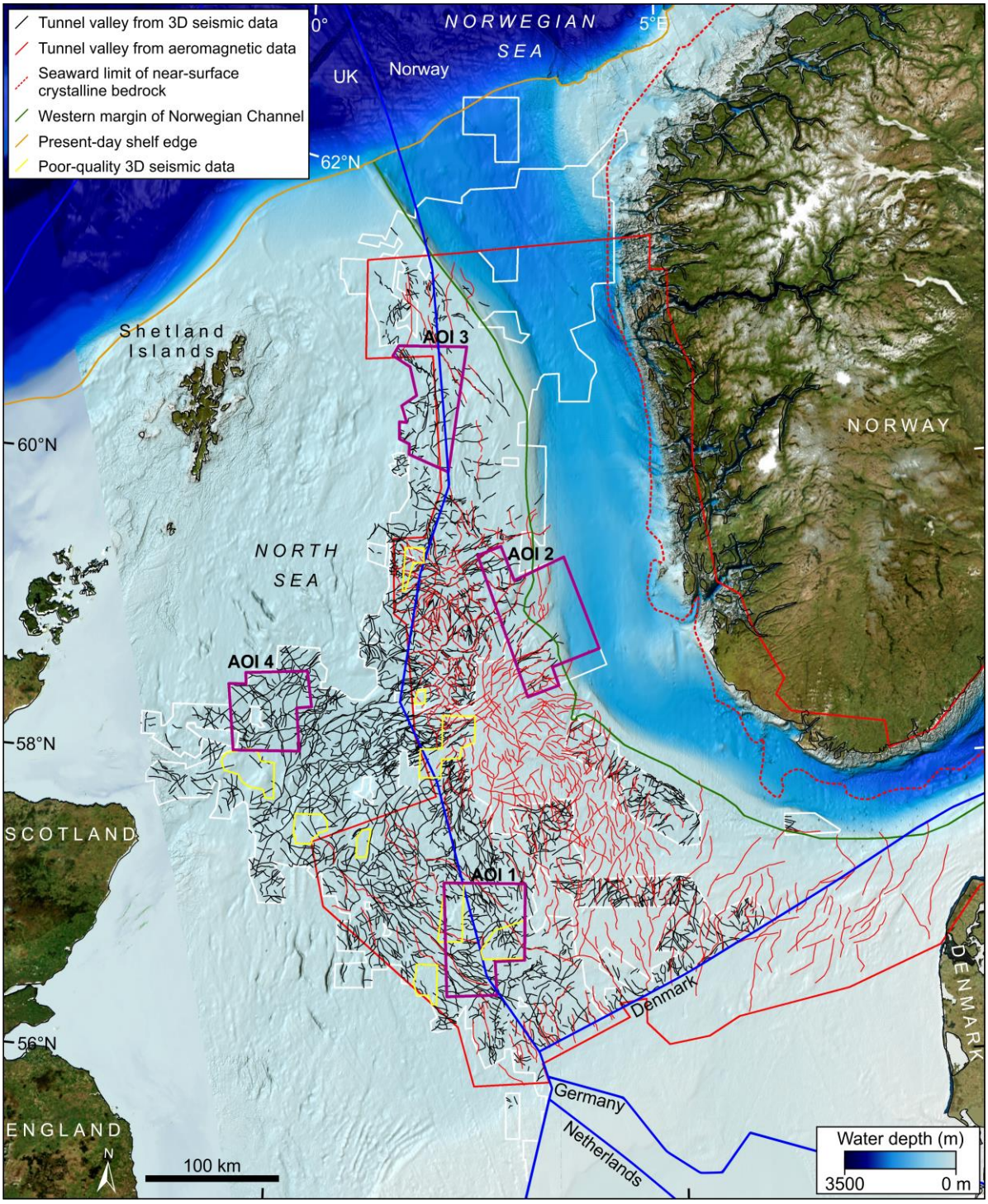
Tunnel valley from 3D seismic data
Tunnel valley from aeromagnetic data
Seaward limit of near-surface crystalline bedrock
Western margin of Norwegian Channel
Present-day shelf edge
Poor-quality 3D seismic data
NORWEGIAN SEA
UK
Norway
0°
5°E
62°N
60°N
58°N
56°N
Shetland Islands
AOI 1
AOI 2
AOI 3
AOI 4
NORTH SEA
NORWAY
SCOTLAND
ENGLAND
Denmark
Germany
Netherlands
DENMARK
100 km
N
Water depth (m)
3500
0 m

Figure 4

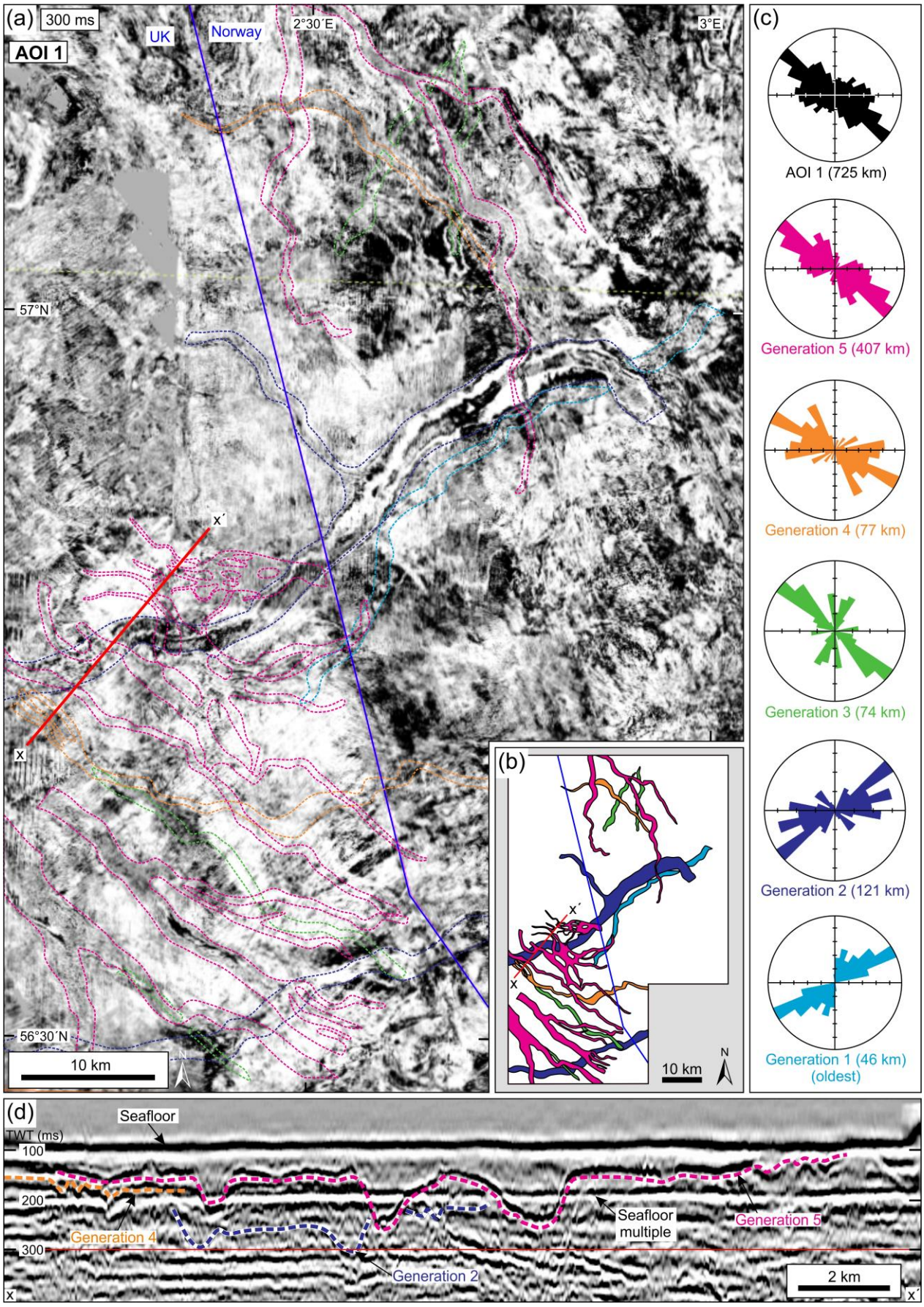
(a)
300 ms
AOI 1
UK
Norway
2°30´E
3°E
57°N
56°30´N
x´
x
10 km
(b)
x´
x
10 km
N
(c)
AOI 1 (725 km)
Generation 5 (407 km)
Generation 4 (77 km)
Generation 3 (74 km)
Generation 2 (121 km)
Generation 1 (46 km)
(oldest)
(d)
Seafloor
TWT (ms)
100
200
300
Generation 4
Generation 2
Seafloor
multiple
Generation 5
2 km
x
x´

Figure 5

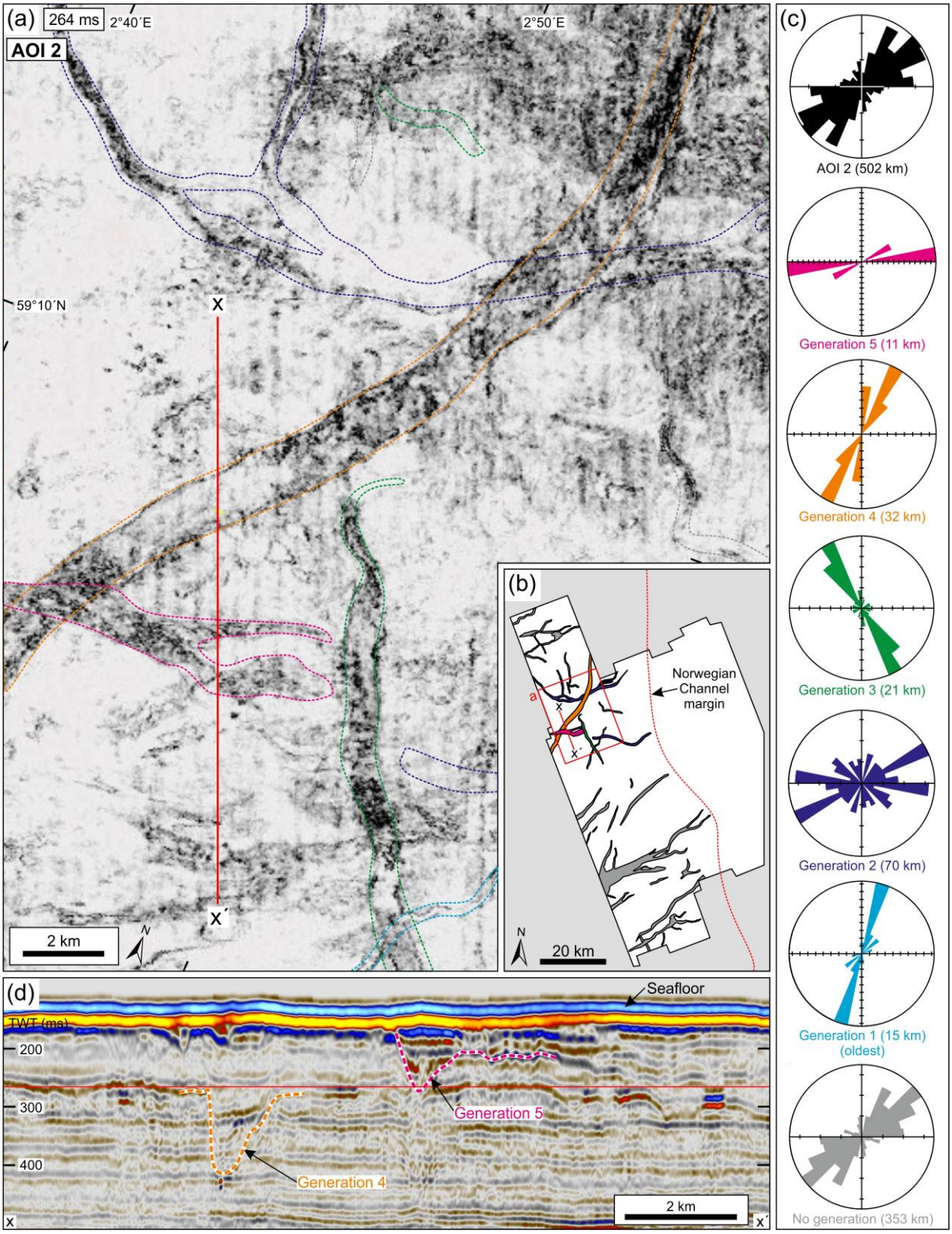
(a)
264 ms
2°40´E
2°50´E
AOI 2
59°10´N
X
X´
2 km
N
(b)
Norwegian
Channel
margin
a
x
x´
N
20 km
(c)
AOI 2 (502 km)
Generation 5 (11 km)
Generation 4 (32 km)
Generation 3 (21 km)
Generation 2 (70 km)
Generation 1 (15 km)
(oldest)
No generation (353 km)
(d)
Seafloor
TWT (ms)
200
300
400
Generation 5
Generation 4
2 km
x
x´

Figure 6

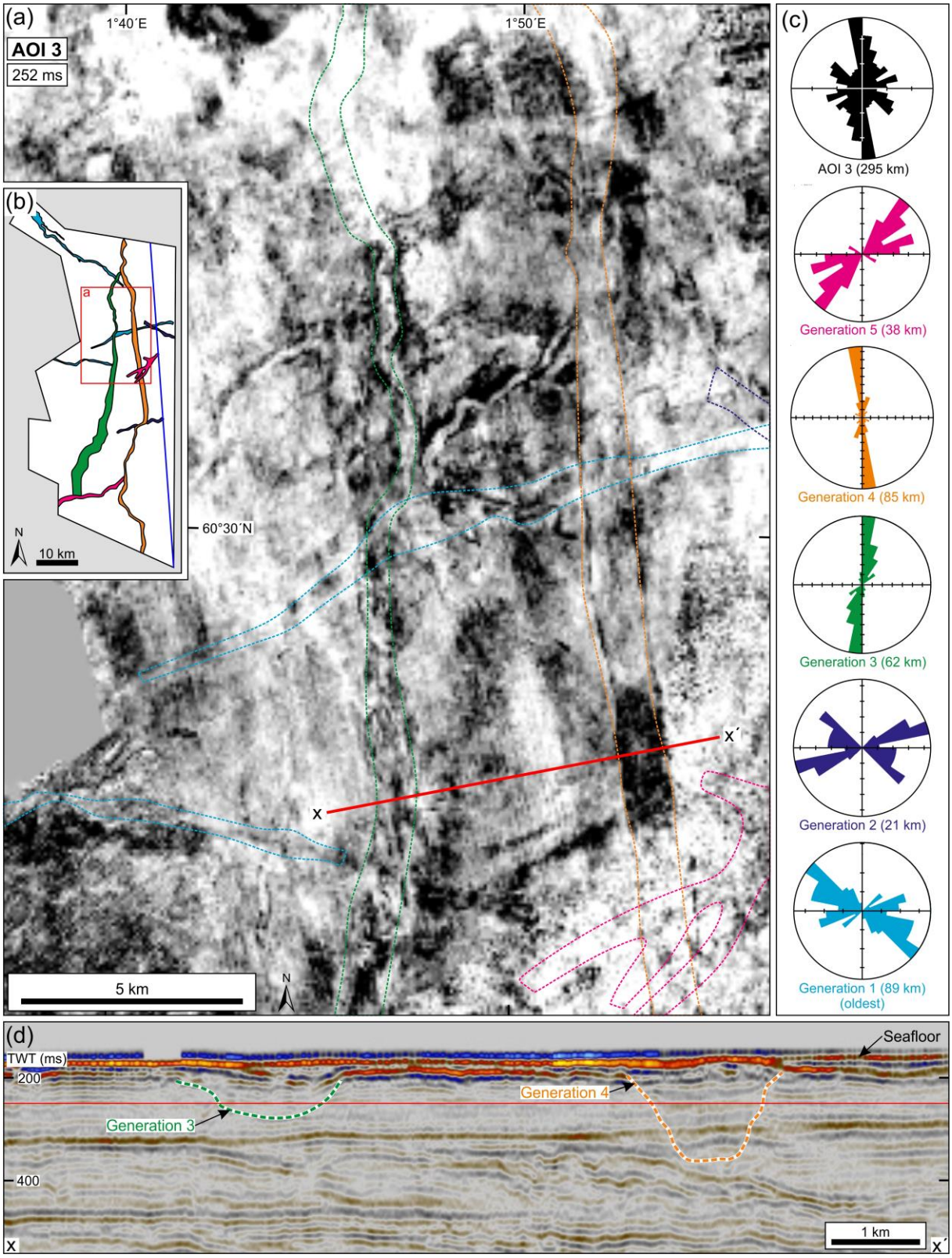
(a)
AOI 3
252 ms
1°40´E
1°50´E
60°30´N
(b)
a
N
10 km
5 km
N
X
X´
(c)
AOI 3 (295 km)
Generation 5 (38 km)
Generation 4 (85 km)
Generation 3 (62 km)
Generation 2 (21 km)
Generation 1 (89 km)
(oldest)
(d)
TWT (ms)
200
400
Seafloor
Generation 4
Generation 3
1 km
X
X´

Figure 7

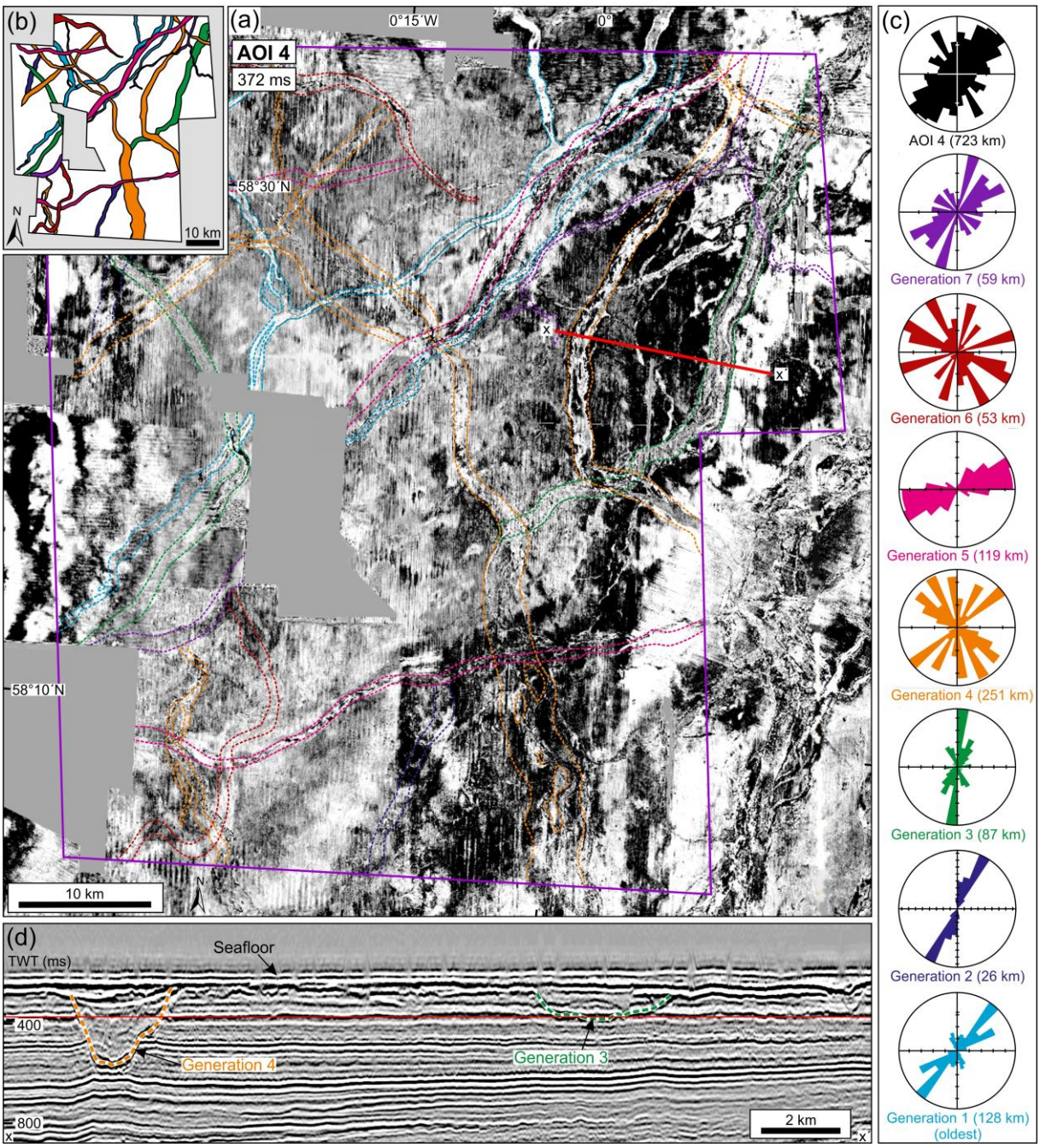
(b)
N
10 km
(a)
0°15´W
0°
AOI 4
372 ms
58°30´N
58°10´N
x
x´
10 km
N
(c)
AOI 4 (723 km)
Generation 7 (59 km)
Generation 6 (53 km)
Generation 5 (119 km)
Generation 4 (251 km)
Generation 3 (87 km)
Generation 2 (26 km)
Generation 1 (128 km)
(oldest)
(d)
TWT (ms)
Seafloor
400
800
Generation 4
Generation 3
2 km
x
x´

Figure 8

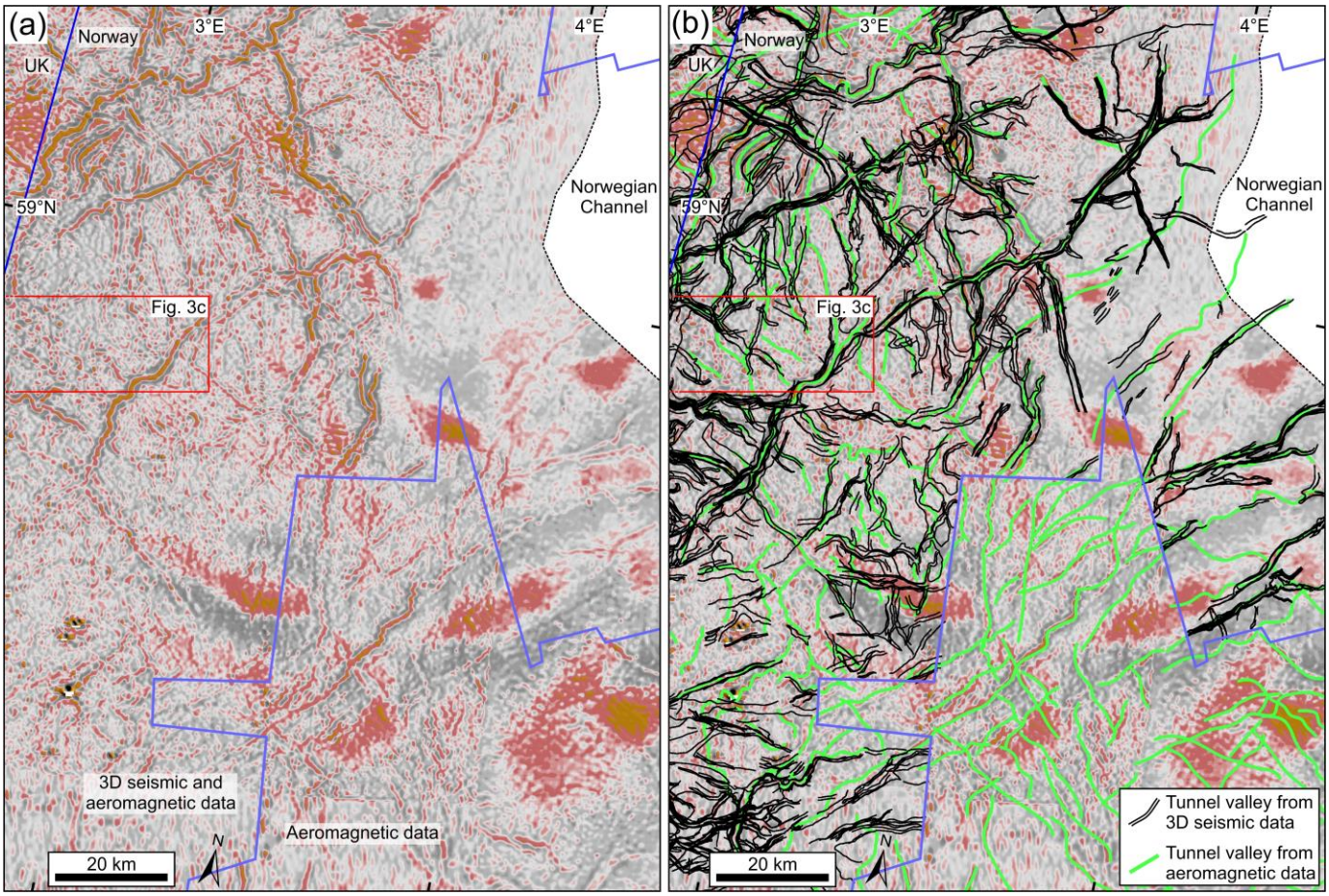
(a)
Norway
UK
3°E
4°E
59°N
Norwegian
Channel
Fig. 3c
3D seismic and
aeromagnetic data
Aeromagnetic data
20 km
N
(b)
Norway
UK
3°E
4°E
59°N
Norwegian
Channel
Fig. 3c
20 km
N
Tunnel valley from
3D seismic data
Tunnel valley from
aeromagnetic data

Figure 9

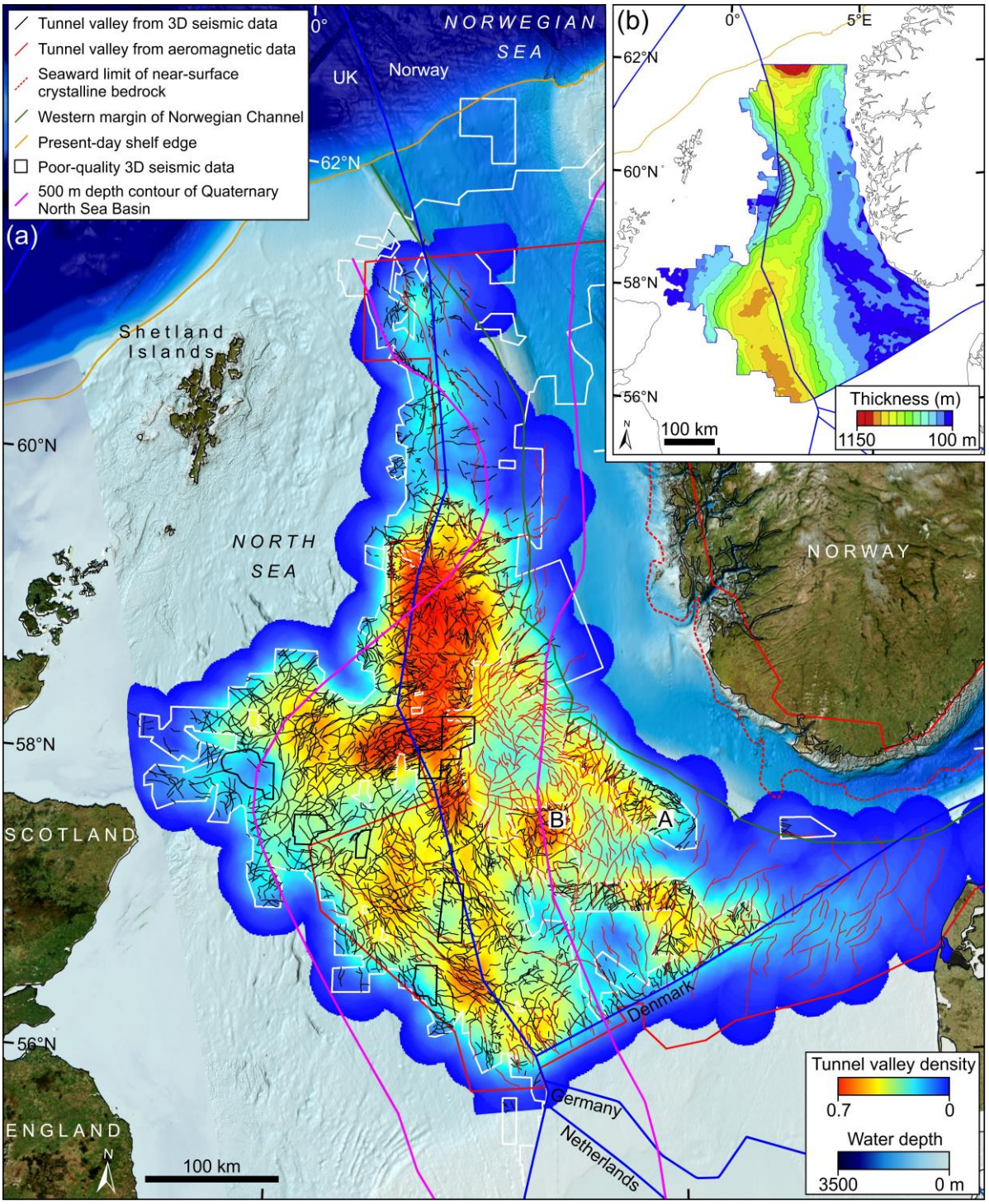
Tunnel valley from 3D seismic data
Tunnel valley from aeromagnetic data
Seaward limit of near-surface crystalline bedrock
Western margin of Norwegian Channel
Present-day shelf edge
Poor-quality 3D seismic data
500 m depth contour of Quaternary North Sea Basin
(a)
(b)
NORWEGIAN SEA
UK
Norway
Shetland Islands
NORTH SEA
NORWAY
SCOTLAND
ENGLAND
Denmark
Germany
Netherlands
A
B
0°
5°E
62°N
60°N
58°N
56°N
100 km
Thickness (m)
1150
100 m
Tunnel valley density
0.7
0
Water depth
3500
0 m

Figure 10

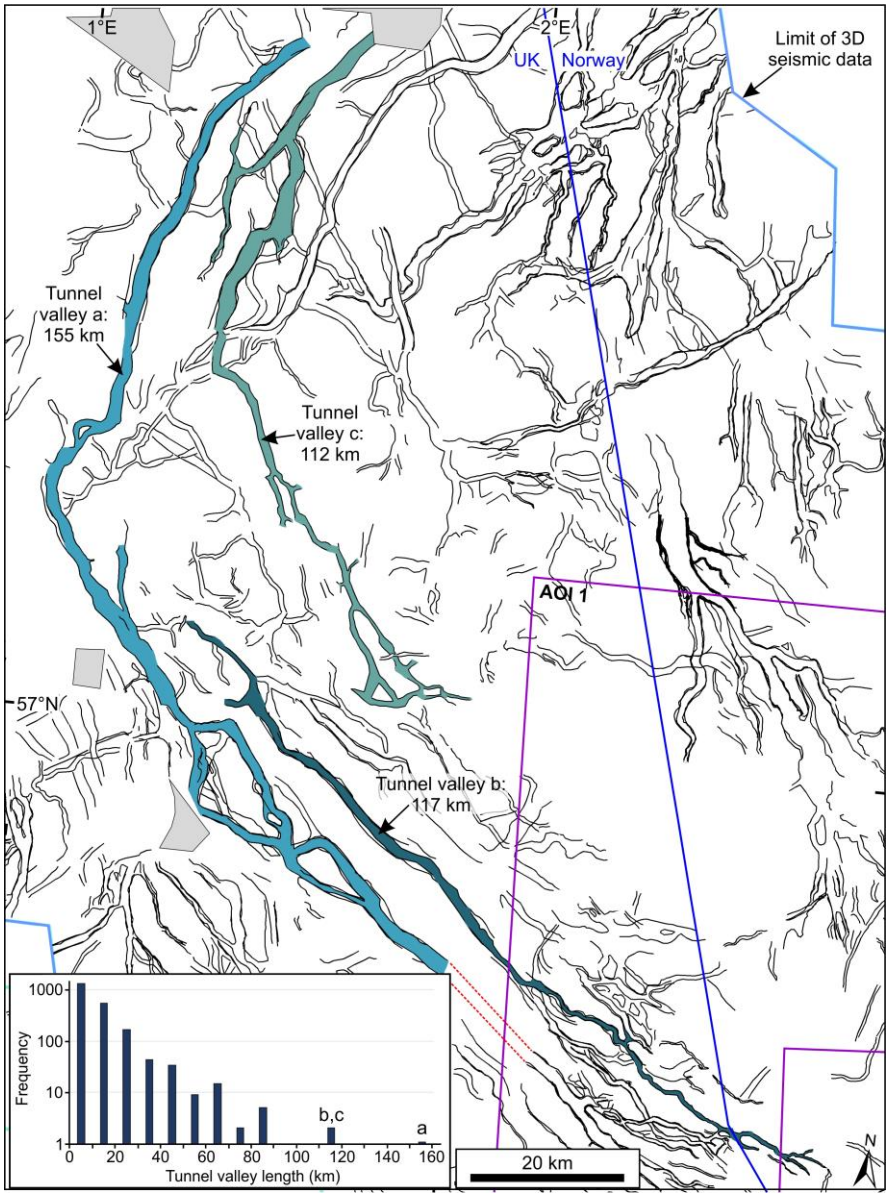
1°E
2°E
UK
Norway
Limit of 3D seismic data
Tunnel valley a: 155 km
Tunnel valley c: 112 km
Tunnel valley b: 117 km
AOI 1
57°N
Frequency
1000
100
10
1
0
20
40
60
80
100
120
140
160
b,c
a
Tunnel valley length (km)
20 km
N

Figure 11

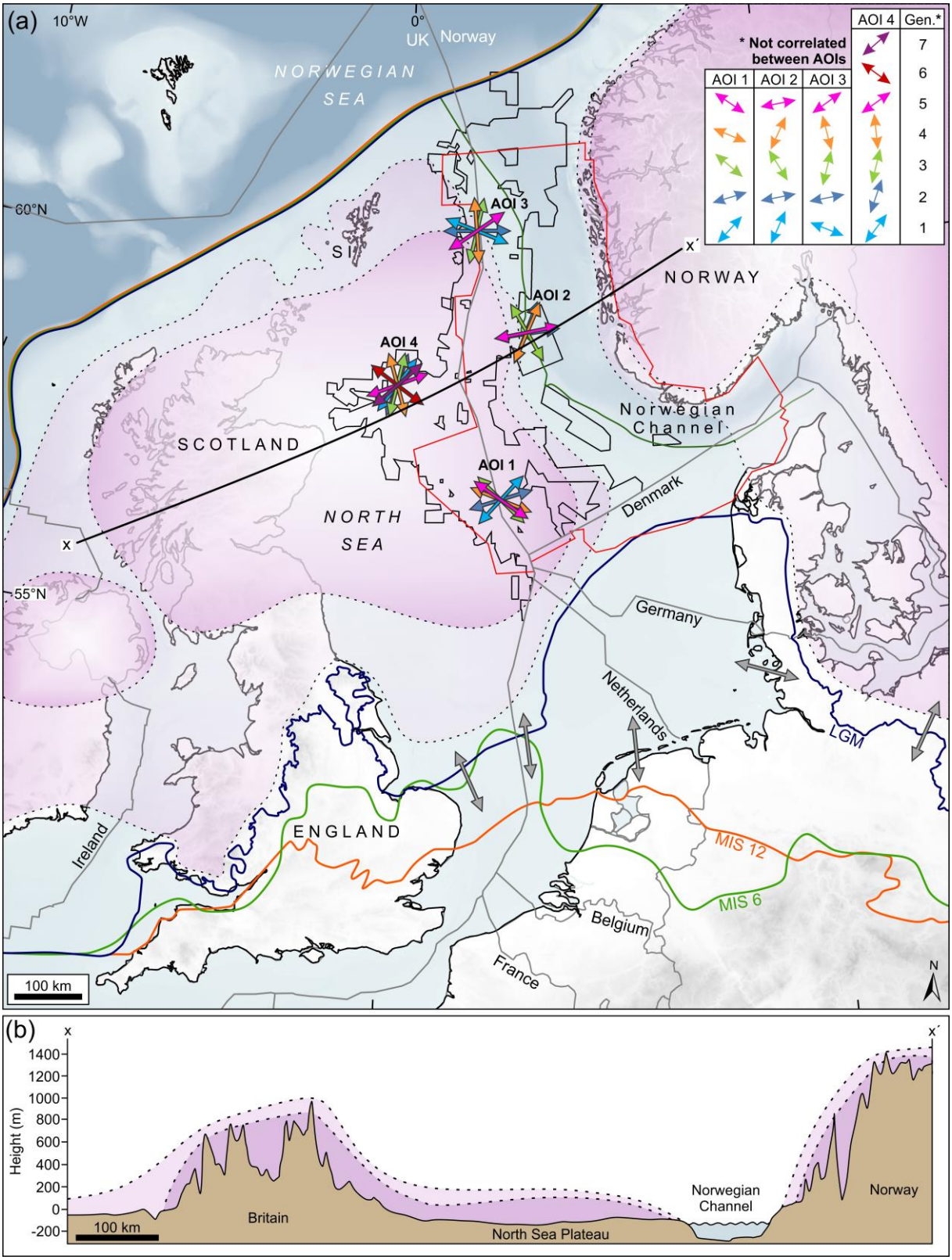
(a)
10°W
0°
UK
Norway
NORWEGIAN SEA
60°N
55°N
SCOTLAND
NORTH SEA
ENGLAND
Ireland
NORWAY
Norwegian Channel
Denmark
Germany
Netherlands
Belgium
France
LGM
MIS 12
MIS 6
AOI 1
AOI 2
AOI 3
AOI 4
x
x´
* Not correlated between AOIs
AOI 1
AOI 2
AOI 3
AOI 4
Gen.*
7
6
5
4
3
2
1
100 km
N
(b)
Height (m)
1400
1200
1000
800
600
400
200
0
-200
Britain
North Sea Plateau
Norwegian Channel
Norway
100 km

Figure 12